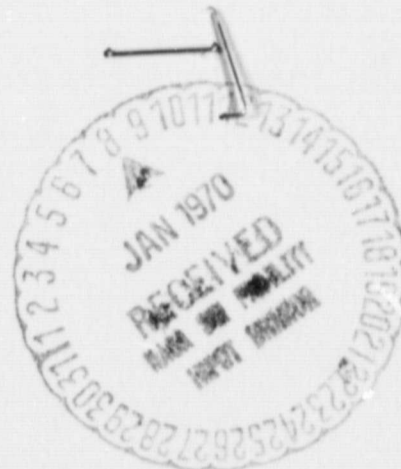


## General Disclaimer

### One or more of the Following Statements may affect this Document

- This document has been reproduced from the best copy furnished by the organizational source. It is being released in the interest of making available as much information as possible.
- This document may contain data, which exceeds the sheet parameters. It was furnished in this condition by the organizational source and is the best copy available.
- This document may contain tone-on-tone or color graphs, charts and/or pictures, which have been reproduced in black and white.
- This document is paginated as submitted by the original source.
- Portions of this document are not fully legible due to the historical nature of some of the material. However, it is the best reproduction available from the original submission.

# RESEARCH REPORT



**N70-27360**

(ACCESSION NUMBER)	(THRU)
63	1
(PAGES)	(CODE)
CR-102658	18
(NASA CR OR TMX OR AD NUMBER)	(CATEGORY)



## BATTELLE MEMORIAL INSTITUTE

COLUMBUS LABORATORIES

SO 759429

ANNUAL REPORT

on

PREDICTION OF SERVICE LIFE OF POLYMERIC  
SEALANT COMPOSITIONS FOR FUEL TANKS IN  
AEROSPACE STRUCTURES FROM MEASURE-  
MENTS OF VISCOELASTIC PROPERTIES

to

NATIONAL AERONAUTICS AND  
SPACE ADMINISTRATION  
GEORGE C. MARSHALL SPACE FLIGHT CENTER  
HUNTSVILLE, ALABAMA 35813

August, 1969

Contract No. NAS8-21398

by

John A. Hassell, Kenneth A. Boni,  
Henry W. Kuhlmann, and E. R. Mueller

BATTELLE MEMORIAL INSTITUTE  
Columbus Laboratories  
505 King Avenue  
Columbus, Ohio 43201

TABLE OF CONTENTS

	<u>Page</u>
INTRODUCTION . . . . .	1
EXPERIMENTAL PROGRAM . . . . .	4
Sealant Preparation . . . . .	4
Weight and Volume . . . . .	6
Shore Hardness . . . . .	6
Tensile and Stress Relaxation. . . . .	6
Torsional Damping . . . . .	7
Aging Equipment . . . . .	7
Single Lap Shear . . . . .	11
RESULTS AND DISCUSSION . . . . .	12
Weight, Volume, and Shore Hardness . . . . .	12
Viton . . . . .	19
Dow Corning 94-030 . . . . .	20
Dow Corning 94-516 . . . . .	20
Tensile and Stress Relaxation. . . . .	20
Viton . . . . .	27
Dow Corning 94-030 . . . . .	29
Dow Corning 94-516 . . . . .	29
Torsional Damping . . . . .	30
Adhesion. . . . .	34
Factors Related to Sealant Performance . . . . .	34
Volume Changes in the Faying Sealant . . . . .	36
Volume Changes in the Filletting Sealant . . . . .	38
Substrate Movements for Both Joint Configurations . . . . .	39
Temperature Induced Strains for Both Joint Configurations . . . . .	40
CONCLUSIONS AND RECOMMENDATIONS . . . . .	41
APPENDIX A . . . . .	A-1
APPENDIX B - TORSIONAL DAMPING EQUATIONS . . . . .	B-1

LIST OF TABLES

Table 1. Compounding Recipe for the Viton Sealant. . . . .	3
Table 2. Structure and Curing Reaction of Dow Corning Sealants . . . . .	3
Table 3. Properties of Unaged Sealants . . . . .	12
Table 4. Initial Measurement of Sealants in Single Lap Shear on Ti-6Al-4V . . . . .	34
Table 5. Tensile Strains Produced by Volume Changes in Faying Sealant . . . . .	38

LIST OF TABLES  
(Continued)

	<u>Page</u>
Table A-1. Certificate of Analysis . . . . .	A-1
Table A-2. Effect of Aging on Tensile Properties of Viton Sealant . . . . .	A-2
Table A-3. Effect of Aging on Stress Relaxation of Viton Sealant . . . . .	A-4
Table A-4. Effect of Aging on Tensile Properties of Dow Corning Sealant 94-030 . . . . .	A-6
Table A-5. Effect of Aging on Stress Relaxation of Dow Corning Sealant 94-030 . . . . .	A-8
Table A-6. Effect of Aging on Tensile Properties of Dow Corning Sealant 94-516 . . . . .	A-9
Table A-7. Effect of Aging on Stress Relaxation of Dow Corning Sealant 94-516 . . . . .	A-11

LIST OF FIGURES

Figure 1. Vapor Pressure of Jet Fuels . . . . .	5
Figure 2. Microtensile-Specimen Die . . . . .	6
Figure 3. The Free Oscillation Arrangement. . . . .	8
Figure 4. Oscillographic Tracings of Damped Oscillations . . . . .	9
Figure 5. Furnace and Bomb for Aging Sealants . . . . .	10
Figure 6. Changes in Weight, Volume, and Shore Hardness of Viton Sealant as a Function of Time in Various Environments (Disk Specimens) . . . . .	13
Figure 7. Changes in Weight, Volume, and Shore Hardness of Viton Sealant as a Function of Time in Various Environments (Microtensile Specimens). . . . .	14
Figure 8. Changes in Weight, Volume, and Shore Hardness of Sealant 94-030 (Lot 911018) as a Function of Time in Various Environments (Disk Specimens). . . . .	15
Figure 9. Changes in Weight, Volume, and Shore Hardness of Sealant 94-030 (Lot 911219) as a Function of Time in Various Environments (Microtensile Specimens) . . . . .	16
Figure 10. Changes in Weight, Volume, and Shore Hardness of Sealant 94-516 (Lot 901205) as a Function of Time in Various Environments (Disk Specimens). . . . .	17

LIST OF FIGURES  
(Continued)

	<u>Page</u>
Figure 11. Changes in Weight, Volume, and Shore Hardness of Sealant 94-516 (Lot 002242) as a Function of Time in Various Environments (Microtensile Specimens) . . . . .	18
Figure 12. Changes in Tensile Properties of the Viton Sealant Aged in Various Environments . . . . .	21
Figure 13. Changes in the Stress-Relaxation Properties of Viton Sealant Aged in Various Environments . . . . .	22
Figure 14. Changes in the Tensile Properties of the Dow Corning 94-030 Sealant Aged in Various Environments . . . . .	23
Figure 15. Changes in Stress-Relaxation Properties of Dow Corning 94-030 Sealant Aged in Various Environments . . . . .	24
Figure 16. Changes in Tensile Properties of the Dow Corning 94-516 Sealant Aged in Various Environments . . . . .	25
Figure 17. Changes in Stress-Relaxation Properties of Dow Corning 94-516 Sealant Aged in Various Environments . . . . .	26
Figure 18. Typical Tensile Load-Time Curve for Viton Sealant . . . . .	28
Figure 19. Effect of Compressive Stress on the Natural Frequency During Torsional Damping . . . . .	30
Figure 20. Effect of Cure on the Torsional Damping Frequency of Sealant 94-516 . . . . .	32
Figure 21. Effect of Cure on the Torsional Damping Complex Modulus of Sealant 94-516 . . . . .	33
Figure 22. Faying Configuration . . . . .	35
Figure 23. Surface of the Sealant in a Faying Configuration Before and After Shrinking . . . . .	35
Figure 24. Filleting Seal Configuration . . . . .	35
Figure 25. Separation of Filleting Seal Into Volume Elements. . . . .	35

## ABSTRACT

This report summarizes a study made to develop test methods aimed at the prediction of service life of polymeric sealant compositions for fuel tanks in aerospace structures from measurements of viscoelastic properties under NASA Contract NAS8-21398.

The effects of aging on various rheological and physical properties of three representative sealants were measured. The properties chosen for measurement were: (1) weight and volume, (2) Shore A hardness, (3) tensile strength and stress relaxation, (4) torsional damping, and (5) single lap shear strength. The changes in these properties, caused by aging of the sealants in various environments and temperatures, were used to determine the mechanisms of sealant degradation that would lead to a fuel leak. Aging of all three sealants in fuel indicates that at least two mechanisms of aging are occurring (and that a simple empirical or theoretical rate equation will not describe these mechanisms).

An analysis of the possible stresses and strains that may be expected in a fuel tank configuration reveals that stresses and elongations are large enough so that rupture of cohesive or adhesive bonds can occur. A critical factor related to a fuel leak is the rate at which these tears or cracks propagate.

Recommendations for a continuation of this study are made to (1) obtain more rheological and physical measurements to help identify additional factors related to the effect of sealant composition on performance, and (2) to investigate simulated service tests for the announced overall purpose, the prediction of service life of sealants.

PREDICTION OF SERVICE LIFE OF POLYMERIC  
SEALANT COMPOSITIONS FOR FUEL TANKS IN  
AEROSPACE STRUCTURES FROM MEASURE-  
MENTS OF VISCOELASTIC PROPERTIES

by

John A. Hassell, Kenneth A. Boni,  
Henry W. Kuhlmann, and E. R. Mueller

INTRODUCTION

Advances in the speed of aircraft have imposed increasingly severe requirements on the materials from which they are fabricated. Tremendous advances in alloys have made the high-speed jet a reality. Currently, large supersonic passenger jets are being designed. One requirement of these jets is a fuel-tank sealant with a 50,000-hour service life in JP-4 type fuels at temperatures from -50 to 500 F (260 C). As a result of this need, NASA is supporting a program aimed at developing such a sealant.

The overall program was divided into three tasks:

- Task A. The Development of New High-Temperature Polymer Systems of Potential Sealant Interest
- Task B. The Formulation, Application, Evaluation, and Process Engineering of New Sealant Materials
- Task C. Prediction of Service Life of Polymeric Sealant Compositions for Fuel Tanks in Aerospace Structure from Measurement of Viscoelastic Properties.

This report describes the work performed at Battelle's Columbus Laboratories on Task C which is aimed primarily at development of short-term tests based on rheological and physical properties of sealants. Prediction of the service life of sealants for aerospace fuel tanks requires establishment of reliable, but relatively short-term, tests that can be used to evaluate the performance characteristics of the sealants. Appropriate tests can be based on changes in physical and rheological properties or a simulation of service conditions.

The approach based on physical and rheological properties is preferred because it relates to identification of the chemical and structural changes produced by aging, information vital to Tasks A and B. Such an approach is also preferred because it will provide information that can be used for predicting service life and failure mechanism of the sealant in a variety of joint and sealant geometries. A simulation test generates data specific to the sealant geometry which it resembles. However, application of data indicating changes in properties resulting from aging to the prediction of service life requires establishment of minimal properties, i.e., those properties required to maintain a seal. The reliability of prediction of minimal properties depends on the accuracy of the prediction of joint and sealant geometries, the expected strain history, and the thermal and chemical environment of the sealant.



The principal effort in this program was aimed at development of reliable measurements of the effects of aging on physical and rheological properties. Properties measured were: (1) weight and volume, (2) Shore A hardness, (3) tensile and stress relaxation, (4) torsional damping, and (5) single lap shear strength.

Changes in weight and volume indicate the nature of interactions with the fuel, i. e., swelling, extraction, or shrinking. The mechanical properties of a sealant will usually vary as the volume changes. Observing the simultaneous changes in volume and mechanical properties can give clues to the possible mechanisms involved in these changes. For example, a small increase in volume accompanied by a large decrease in Young's modulus would indicate that bonds have been ruptured. Volume changes themselves can lead to both cohesive and adhesive failures. Change in weight indicates whether volume changes are accompanied by gain or loss of material.

The Shore hardness test is a simple, rapid method of determining the hardness of polymeric materials. The number obtained is related to the modulus and will change as bonds are formed or broken. When the Shore hardness varies during the measurement, it reflects the stress-relaxation characteristics of the material.

Tensile tests are used universally for determining the strength and deformation of materials. Moduli, stress, and strain data obtained from such tests are useful in characterizing materials before and after exposure to various environmental conditions. The stress-relaxation test is used to measure time-dependent characteristics of materials and is described as the decay of stress with time at constant elongation. The rate at which the stress decays is a function of polymer composition and structure, and is known to change with aging. Both tensile and stress-relaxation measurements are useful as means of characterizing the viscoelastic behavior of sealants.

Torsional damping provides a dynamic nondestructive measurement that can be used to determine the amount of damping or viscous loss. With appropriate models, the damping of the material can be expressed in terms of viscous and elastic moduli. The viscous or loss modulus is related to the energy lost as heat; the elastic modulus is related to the elastic or recoverable energy. The torsional-damping test requires small deformations, and thus should not cause significant cumulative damage to a material. Since it is a nondestructive test, cumulative aging effects on a single specimen can be obtained. Therefore, fewer specimens are required than for tensile tests. By varying the frequency of the oscillation, time-dependent effects can be determined. This measurement duplicates more readily the type of motion to which the sealant would be subjected during actual flight in an integrated wing tank. The moduli obtained can be used in predicting the stress levels resulting from a deformation, along with indications of the time dependence of these moduli as derived from their frequency dependence.

The seal can fail cohesively or adhesively. The same sealant degradation mechanism may or may not be responsible for both types of failure. Two types of adhesion tests are widely used to characterize the adhesive characteristics of sealants, the lap shear test and the peel test. Only the lap shear test was used in the current program.

Three representative sealants were studied in this program, a Viton sealant, and Dow Corning's 94-030 and 94-516 sealants. The Viton sealant was prepared by W. Anspach of WPAFB (MANE) and submitted to Battelle in tensile sheet form (~0.07 inch thick). The compounding recipe of this sealant is given in Table 1.

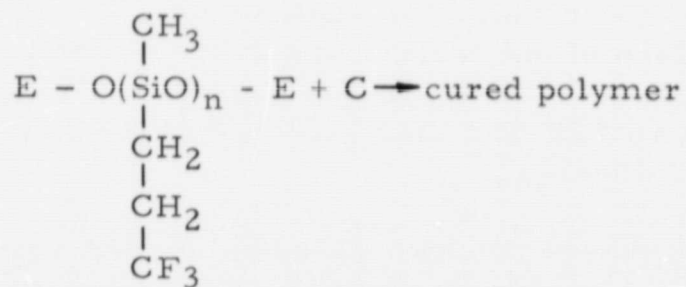
TABLE 1. COMPOUNDING RECIPE FOR THE VITON SEALANT

Material	Parts
Viton B	45
Extracted Viton LM	55
MT Black	15
Maglite Y	15
FS 1265 (1000 CS)	8
MEK	20
Ketimine (Blocked EDA)	2

Viton B is a copolymer prepared from  $\text{CF}_2=\text{CF}-\text{CF}_3$ ,  $\text{CH}_2=\text{CF}_2$ , and  $\text{CF}_2=\text{CF}_2$ , and is crosslinked by extracting HF with an amine. (1)

The Dow Corning sealant designated 94-030 comes packaged in sealed polyethylene cartridges. It cures by reacting with atmospheric water vapor, liberating acetic acid. The other Dow Corning sealant, designated 94-516, is prepared by mixing ten parts of base with one part of curing agent. In preparing this sealant, especially in small batches, extreme caution must be taken to assure that the curing agent is well mixed before adding to the base. The curing agent contains some inert ingredients which can separate and produce nonuniformity in concentration of the active ingredients.

The two Dow Corning sealants have the same polymer structure, but differ in their end groups. The curing reaction is:



where the end groups, curing agent and catalyst are shown in Table 2. Two batches of each of the Dow Corning sealants were used in this work: for 94-030, Lots 911018 and 911219 and for 94-516, Lots 901205 and 002242. The sealant compounding ingredients, except for the polymer, were not revealed to Battelle.

TABLE 2. STRUCTURE AND CURING REACTION OF DOW CORNING SEALANTS

Sealant	End Group (E)	Curing Agent (C)	Catalyst	Bond
94-030	-H	$\text{R}' - \text{Si}(\text{OR})_3^a$	$\text{H}_2\text{O}$	$\begin{array}{c}   \quad   \\ -\text{Si}-\text{O}-\text{Si}-\text{O} \\   \quad   \end{array}$
94-516	$\begin{array}{c}   \\ -\text{Si}-\text{CH}=\text{CH}_2 \end{array}$	$\text{R}' - \text{Si}(\text{OSiMe}_2\text{H})_3$	Pt + Heat	$\begin{array}{c}   \quad   \quad   \quad   \\ -\text{O}-\text{Si}-\text{C}-\text{C}-\text{Si}-\text{O}- \\   \quad   \quad   \quad   \end{array}$

(a) R is an acetoxy group and R' a hydrocarbon group

(1) Barney, A. L., "Chemistry of Fluorocarbon Elastomers", paper presented at Polymer Conference Series, Wayne State University (May, 1966).  
Ebron "Room Temp Curing Reaction of Silicone Resins".

The fuel used in this program was obtained from Ashland of Kentucky. The composition of this fuel, identified as Grade II MIL-J-5161F, is indicated by the analysis shown in Table A-1. The temperature dependence of the vapor pressure, given in Figure 1, was determined at Battelle by measuring the pressure attained at several temperatures in a bomb loaded with fuel.

### EXPERIMENTAL PROGRAM

#### Sealant Preparation

Tensile measurements strongly depend on the uniformity of the sample being tested. Therefore, considerable effort was directed toward preparation of bubblefree, smooth surface, and uniformly thick tensile sheets from which tensile specimens could be cut. Because of the different types of cure for the Dow Corning 94-030 and 94-516 sealants, different procedures are required for preparation of the sheets for tensile-property measurements.

The Dow Corning 94-030 sealant is air cured and comes in Semco polyethylene cartridges. Approximately 100 milliliters of sealant was extruded onto the center of a 4 x 6-inch Teflon sheet which contained two 1/8-inch spacers on the opposite edges. A piece of decal paper (which has a water-soluble surface) was placed, with the water-soluble surface down, on top of the sealant. A roller that extended across the two spacers was used to reduce the sealant "glob" to a uniform 1/8-inch sheet. After curing for 1 week at a constant humidity (about 50 percent), the sealant was peeled off the Teflon sheet and soaked in warm water for approximately 5 minutes before removing the decal paper. The surface of the sealant was rubbed lightly in water with a sponge to remove the water-soluble residue left on the surface. This produced a smooth, non-glossy, flat surface. The sealant was then returned to the constant-temperature room for additional cure of up to 5 weeks.

Dow Corning Sealant 94-516 is a two-part sealant and requires mixing of the curing agent immediately before using. Because of the high viscosity of this sealant, the mixing procedure traps a large amount of air in the sealant. If cast in this state, the resulting sheet is spongy and contains a large number of bubbles. Therefore, the following procedure was used to cast smooth bubblefree sheets.

One part of curing agent was added to ten parts of sealant. This mixture was mixed well in a beaker with a spatula and transferred to a Semco polyethylene cartridge. The cartridge was then placed in a vacuum chamber and evacuated to remove the air. The vacuum had to be broken repeatedly to rupture the bubbles which formed in the sealant. After approximately 15 minutes, most of the air had been removed. The cartridge then was centrifuged in an International centrifuge for 20 minutes at approximately 1,200 g to further reduce the bubble content and position the sealant in the lower end of the cartridge. The bubblefree sealant was extruded onto a smooth steel plate which contained four 1/8-inch spacer dams around the edge. The plate had been cleaned and lightly coated with a mold-release agent. A similar plate was placed on top and the sandwich pressed at approximately 1,000 pounds. This sandwich was placed in an oven at 150 C for 75 minutes. (The recommended cure is 60 minutes, but 15 minutes was allotted for warm-up.)

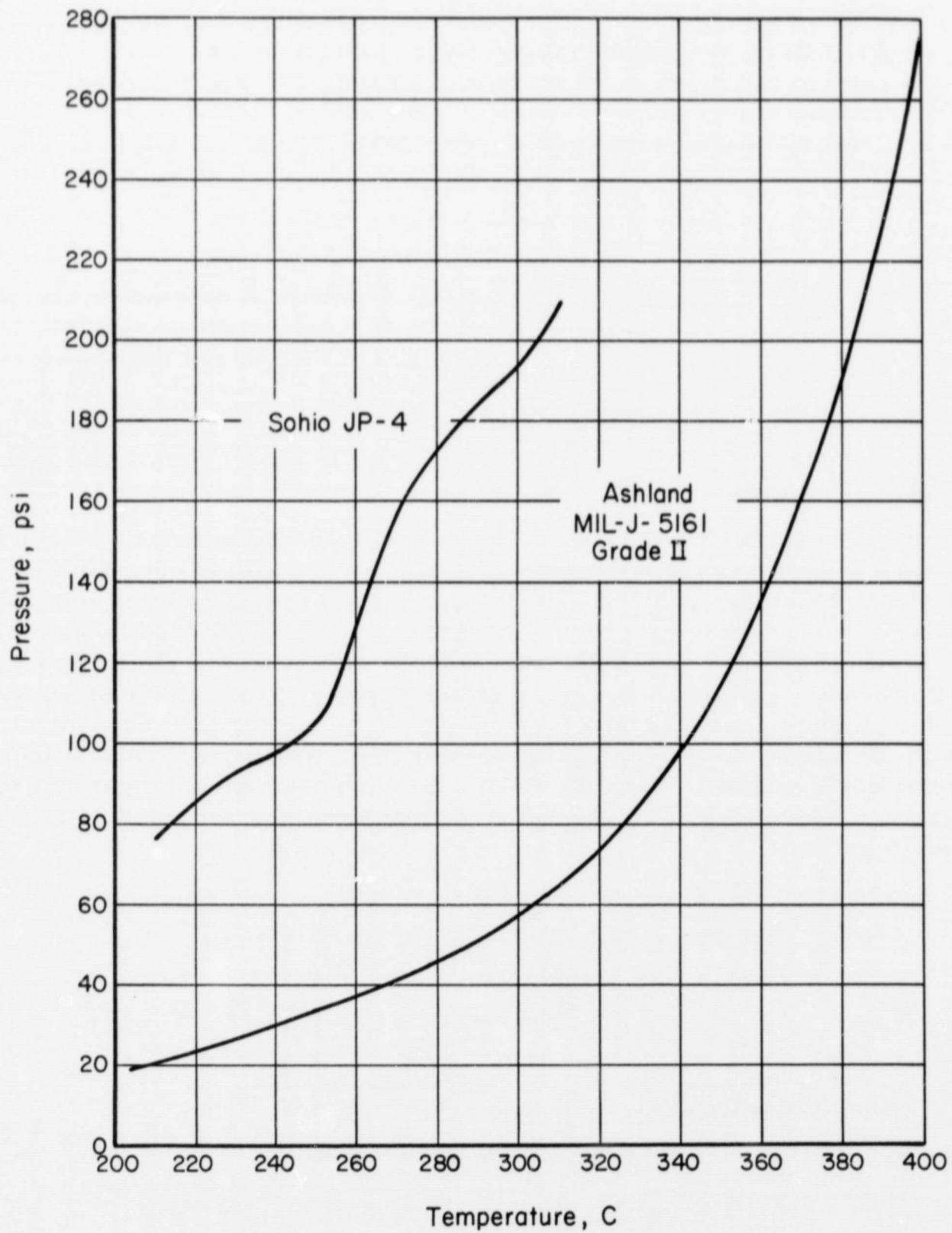


FIGURE 1. VAPOR PRESSURE OF JET FUELS

### Weight and Volume

A "Right A-weigh" analytical balance reliable to  $\pm 0.2$  mg was used in all weighings. The volume was determined from the difference between the weight of specimen in air and that in fuel (Archimedes principle). The weight in fuel was determined by suspending the specimen on a thin copper wire from the hook suspension of the balance. The density of the fuel was measured with a glass hydrometer prior to each set of weighings. All weighings were made in a room with the temperature controlled to  $22.5 \pm 0.5$  C. The weight in air was determined prior to determination of weight in fuel in order to avoid possible errors from fuel clinging to the surface of the sealant. Fuel was removed from specimens aged in fuel by blotting them with a paper towel.

### Shore Hardness

The hardness of the sealants was measured using a Shore A durometer mounted on a Code DRCL operating stand which applied a load of 1,065 grams on the durometer foot. Specimens were stacked to obtain a pile at least 1/4 inch thick. Hardness values observed at 10 seconds were recorded.

### Tensile and Stress Relaxation

Both the tensile and the stress-relaxation tests were performed with a floor model Instron Universal Tester using the microtensile specimen cut with the die illustrated in Figure 2. The tensile test was performed by elongating the specimen at 20 ipm until rupture occurred. The load was recorded on a chart at 50 ipm, and the elongation was determined from the crosshead displacement. In some cases, where the material is soft, the specimen would slip out of the grips before rupture. This was avoided by folding a piece of emery cloth double around the specimen tabs so that the abrasive came in contact with both the specimen tabs and the grip surfaces. The stress-relaxation test was performed by elongating the specimen at 20 ipm to approximately 20 percent of its ultimate elongation. The decay of the load at this elongation was recorded as a function of time for 5 to 15 minutes.

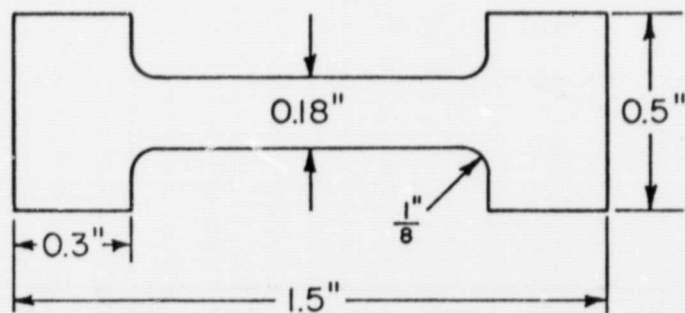


FIGURE 2. MICROTENSILE-SPECIMEN DIE

(Scale 2 inches = 1 inch)

Three microtensile specimens were tested at each aging condition. First, one was pulled to rupture in order to estimate the ultimate elongation. Then stress relaxation was performed on the other two to approximately 20 percent of the ultimate elongation of the first. The tensile properties of the latter specimens were determined at least 16 hours after the stress-relaxation measurement in an effort to minimize the effect of the stress relaxation. The cross section and gage length of the specimens were measured with a Vernier caliper which can be read to  $\pm 0.001$  inch. The elongation during the tensile test was determined from the time axis of the load recording. The specimen elongation during the stress-relaxation test was obtained from the gage-length micrometer of the Instron. The unaged gage length of the specimen was set at 0.8 inch. The actual length was measured between the inside edges of the tab, and this value multiplied by 0.8/0.87 to obtain the gage length. (0.87 was found to be the actual distance between the tabs for the unaged specimen.)

#### Torsional Damping

Torsional damping was performed on a Weissenberg Rheogoniometer using the arrangement shown in Figure 3. Disks of approximately 3/4-inch diameter and from 0.06 to 0.15 inch thick were stacked 2 to 4 high between the two serrated platens of the instrument. The upper platen was lowered until the specimen had been compressed to 98.5 percent of its unstressed height. (This was done to avoid slippage at the specimen-platen interface.) The weights on the inertia arm are first moved to the innermost position for the minimum inertia (maximum frequency) and lightly stroked to start the upper assembly oscillating. The weights were then positioned in the middle and ends of the inertia arm to produce a threefold range of inertia. The amplitude of the oscillation was varied within a 10- to 100-fold range with a maximum shear strain at the outer edge of the disk of 3 percent. Typical damped oscillations are shown in Figure 4. The information obtained from this experiment is the frequency,  $f$ , and the decrement,  $\delta$ , which can be defined by the relation

$$\delta = \frac{1}{n} \ln \frac{A_0}{A_n},$$

where  $A_n$  is the amplitude of the  $n$ th successive cycle after  $A_0$ . The decrement and frequency are then used (see Appendix B) to calculate the viscous and elastic moduli of the material.

#### Aging Equipment

The constructions of the bombs and furnaces used in the aging study are shown in Figure 5. The body of the bomb is 1-1/4-inch carbon steel Schedule 80 pipe with approximately 1-5/8-inch outside diameter, to which is welded a 1-1/4-inch Schedule 80 welding cap. The sealants to be aged in fuel were loaded in 29-mm-OD glass tubes and placed in the bombs with 20 cc of fuel. The glass tubes were used to avoid reactions with the metal bomb. The vapor-aged specimens were suspended over the fuel with glass hooks and a wad of glass wool was placed between the liquid and the specimens to prevent them from dropping into the liquid. The bombs were sealed by placing a light film of Dow Corning silicone stopcock grease on both sides of the washer (lead was used for 150 and 200 C, and copper for 250 C) and tightening the threaded cap. They

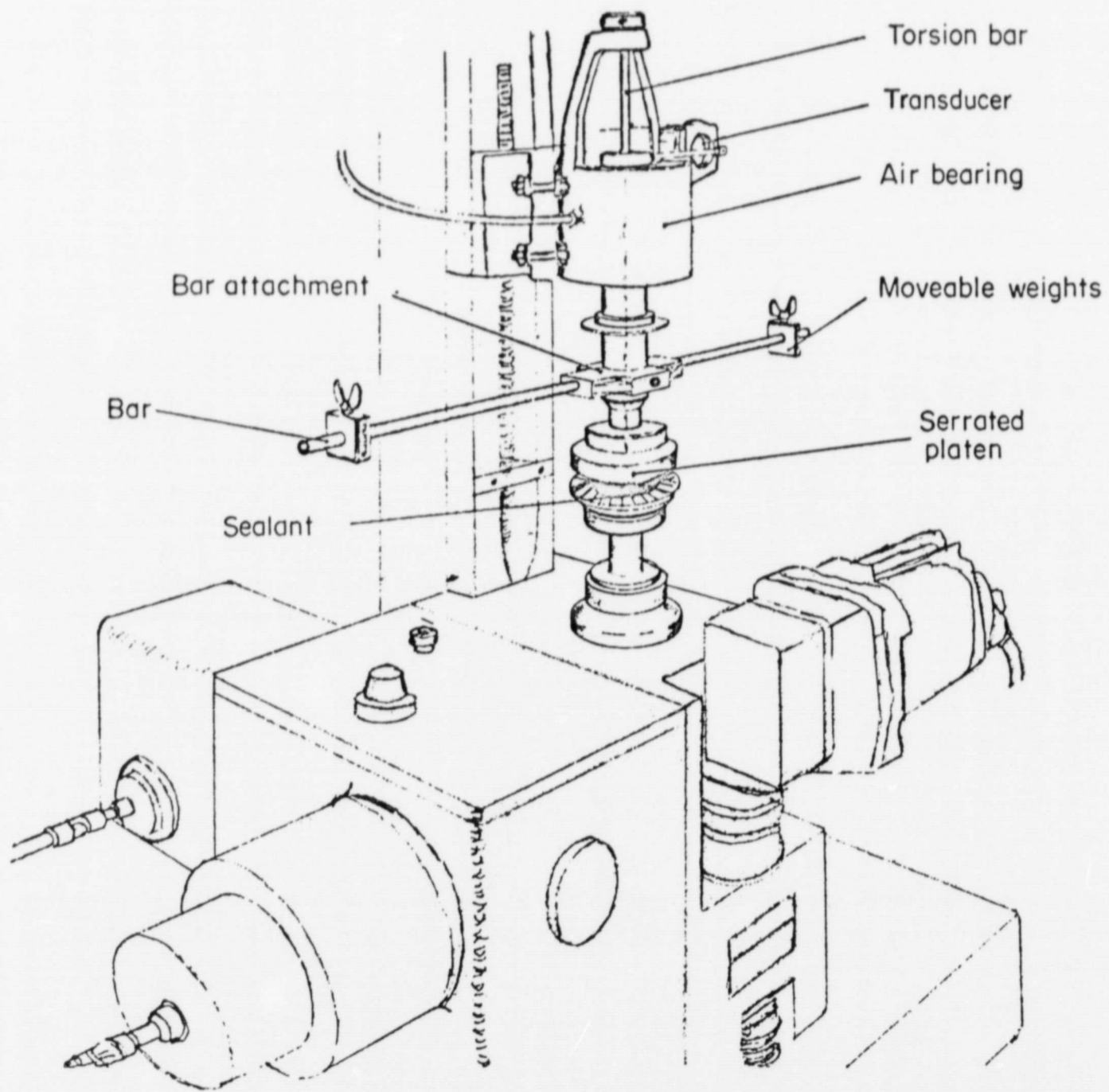


FIGURE 3. THE FREE-OSCILLATION ARRANGEMENT

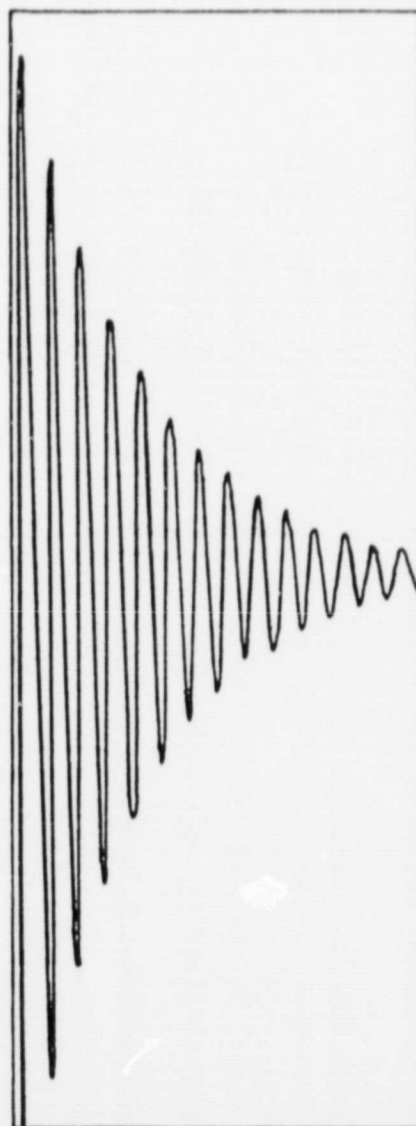
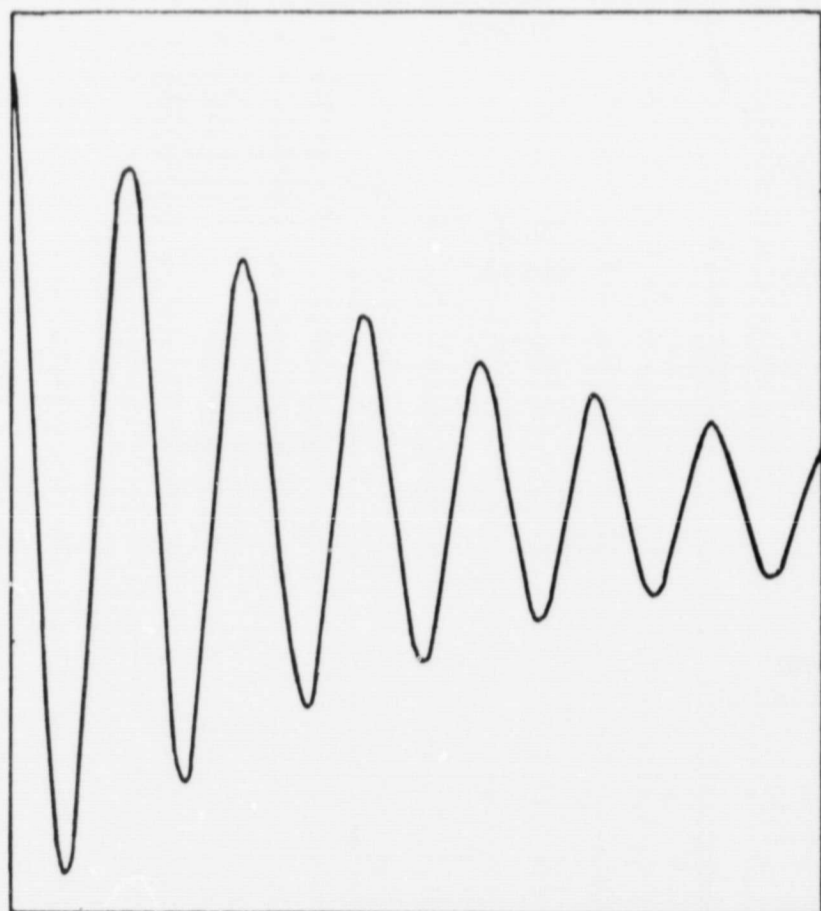


FIGURE 4. OSCILLOGRAPHIC TRACINGS OF DAMPED OSCILLATIONS



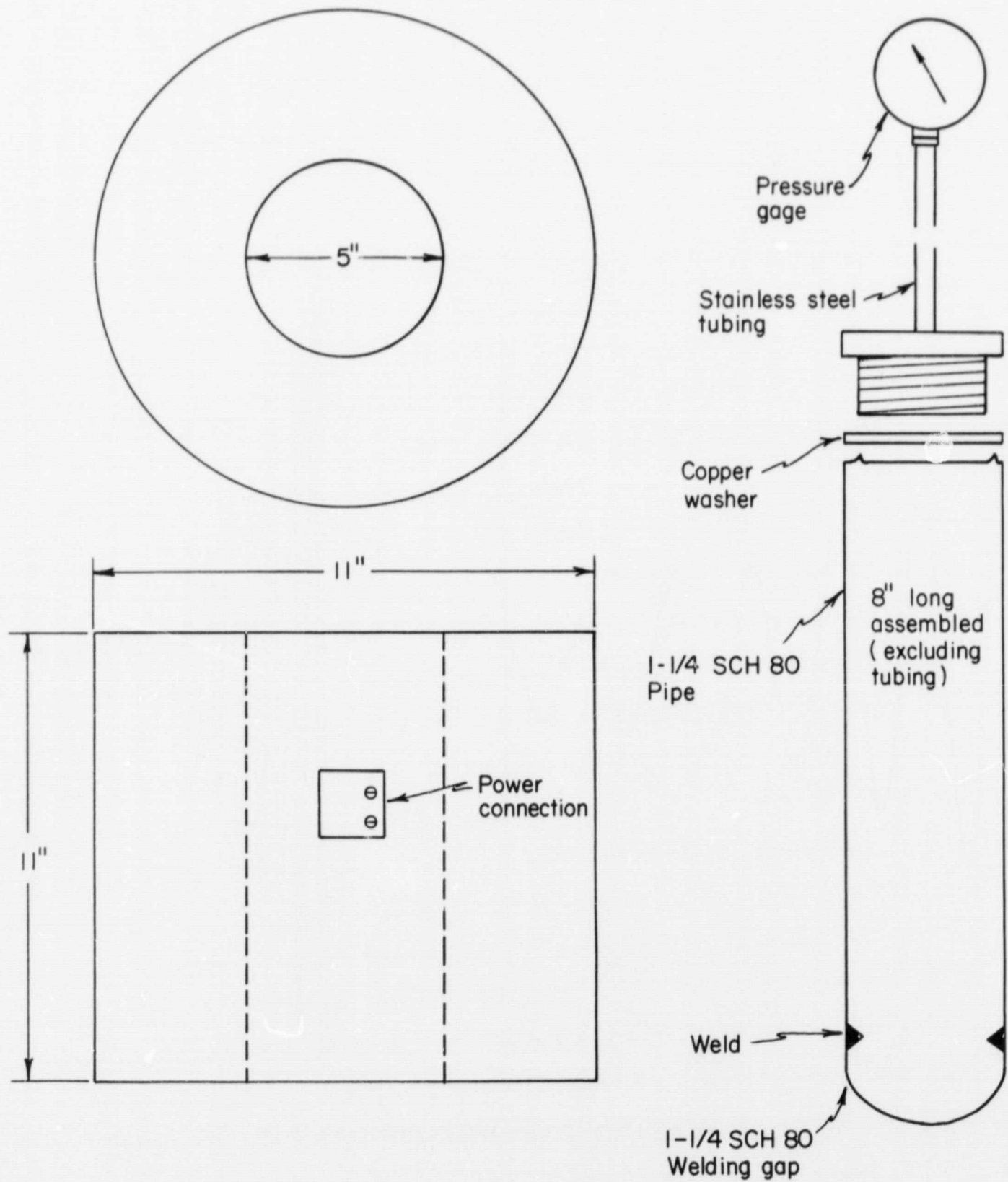


FIGURE 5. FURNACE AND BOMB FOR AGING SEALANTS

were leak tested before use by removing the pressure gage and applying 100 pounds of air pressure on the sealed bombs, immersing them in water, and observing any bubble formation. If, during any prolonged testing, the pressure on the gage dropped to zero, the bomb was removed and resealed. In most instances of aging in fuel for longer than 4 hours, the pressure dropped from its initial value, most likely due to extracted sealant and thermally induced changes in composition of the fuel. Following aging, the volume of fuel was checked to assure negligible leakage.

The furnaces used to heat the bombs were constructed from 5/8-inch wall, 5-inch diameter ceramic tube with a resistance heating wire wound on the outside. Temperature control on these furnaces was obtained in the initial stages of this work by adjusting the current fed to the furnace with a Variac until the desired temperature was achieved. This allowed control to within  $\pm 1$  C at the lower temperatures, but exhibited appreciable day-to-day fluctuation. Two Pak-tronics Model No. 501 proportional controllers fitted with a 2-inch platinum probe were subsequently used for the elevated temperatures. (Aging on all the microtensile specimens, except at 150 C, was carried out using these controllers.) These units controlled to within  $\pm 1$  C for 24 hours and to within  $\pm 2$  C for longer periods of time. They also reduced to 15 minutes the time necessary to achieve equilibrium temperatures after loading of the bombs.

#### Single Lap Shear

Single lap shear specimens were used to evaluate the adhesive properties of the sealants. The lap shear specimens were prepared by cleaning 0.75 inch of the end of a 1.5 x 0.5 inch Ti-6Al-4V tab. The cleaning procedure was:

- (1) Clean off surface with steel wool
- (2) Rub lightly with emery cloth
- (3) Rinse with acetone
- (4) Soak for 15 to 30 minutes in Pasa Gel
- (5) Rinse in tap water followed by distilled water
- (6) Final rinse with acetone and air dry.

A thin coat of primer was then applied to the cleaned surface with an air brush and let dry for 60 to 90 minutes at 22.5 C and 50 percent relative humidity. Half of the prepared tabs were lined up on a flat steel sheet against a metal spacer (to provide 10 to 20-mil sealant thickness). These tabs were clamped on the untreated end with a metal bar and C-clamps. Sealant was applied in a thick ribbon on the center of the prepared surface and the second tab was placed on a spacer with the primed surface down and overlapping the lower tab by 0.5 inch. This upper row was clamped with a metal bar. The curing times and temperatures used were similar to those used during preparation of the tensile sheets.

Aging and testing of these specimens were identical to those of tensile specimens, except that the crosshead speed of the Instron was 0.02 to 0.05 ipm.

## RESULTS AND DISCUSSION

### Weight, Volume, and Shore Hardness

The weight, volume, and Shore hardness of the three sealants were significantly changed by exposing them to air and fuel (liquid or vapor) at or below 250 C as shown in Figures 6 through 11. The method of determining the data shown in Figures 6, 8, and 10 differed from that used to determine the data in Figures 7, 9, and 11 in two ways. First, microtensile specimens rather than disk-shaped specimens were used. Second, data points were obtained from separate sets of specimens rather than from cumulative aging of the same specimens. The principal effect of these procedural changes is to include any variability within a specimen with the changes produced by aging, and residual fuel from the volume determination of air-aged specimens could affect subsequent air-aging data for the disk specimens. In addition to the procedural differences, it should be noted that the two sets of data on each Dow sealant were obtained on different lots.

Identification of experimentally significant changes produced by aging and use of different lots of the same sealant requires establishment of the reliability of measured properties of a single sealant. Results indicating the precision of Shore hardness data are given in Table 3. It was necessary to use more than one specimen for the Shore hardness measurement in order to obtain the minimum requirement of 1/4 inch thickness.

TABLE 3. PROPERTIES OF UNAGED SEALANTS

Sealant	Shore Hardness	Tensile			Stress Relaxation	
		Young's Modulus, psi	Rupture Stress, psi	Elongation, %	Modulus at .05 Min, psi	Slope <sup>(a)</sup>
Viton	54 ± 1.2 <sup>(b)</sup>	1100	455	265	335	86
Dow Corning 94-030 (Lot-911219)	50 ± 1.2 <sup>(b)</sup>	485	575	280	190	19
94-030 (Lot-911018)	44 ± 3.5 <sup>(c)</sup>	-	-	-	-	-
94-516 (Lot-002242)	37 ± 1.8 <sup>(b)</sup>	135	460	235	105	7
94-516 (Lot-901205)	49 ± 2.7 <sup>(d)</sup>	-	-	-	-	-

(a) Slope of the log modulus-log time plot.

(b) Standard deviation of 18 separate measurements; microtensile specimens stacked 3 high.

(c) Standard deviation of 6 separate measurements; disk specimens stacked 2 high.

(d) Standard deviation of 6 separate measurements on single disk specimens.

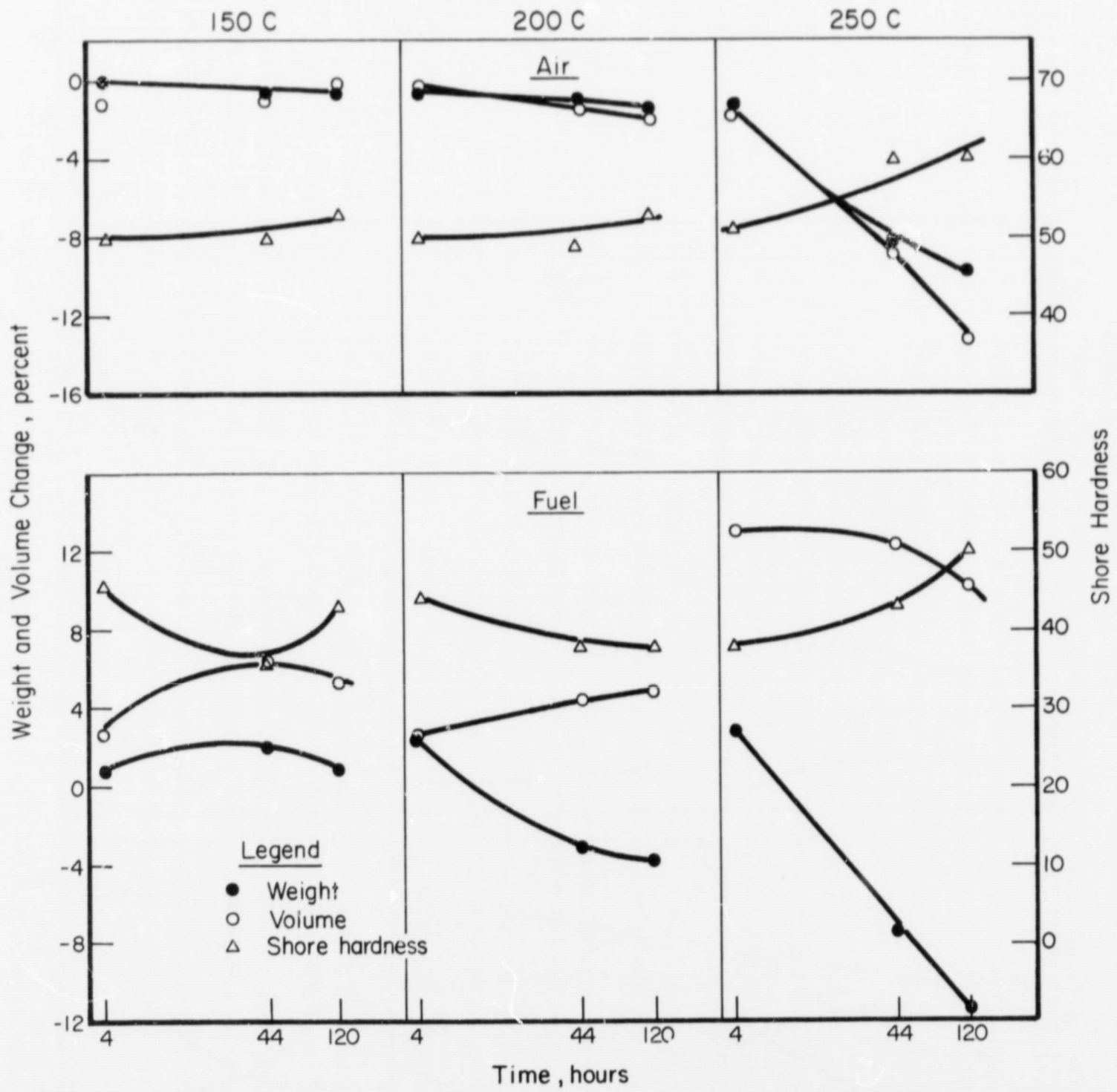


FIGURE 6. CHANGES IN WEIGHT, VOLUME, AND SHORE HARDNESS OF VITON SEALANT AS A FUNCTION OF TIME IN VARIOUS ENVIRONMENTS (DISK SPECIMENS)

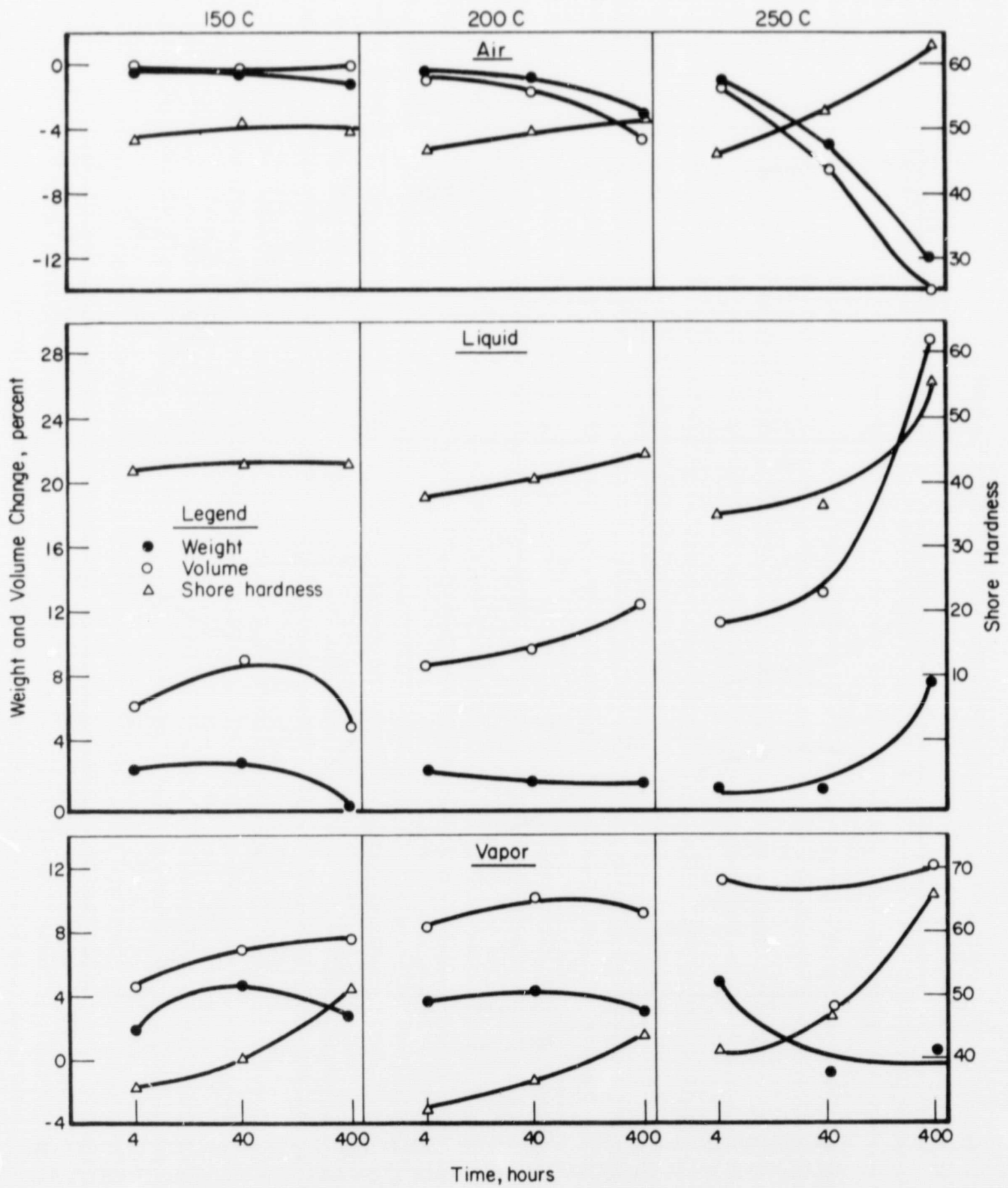


FIGURE 7. CHANGES IN WEIGHT, VOLUME, AND SHORE HARDNESS OF VITON SEALANT AS A FUNCTION OF TIME IN VARIOUS ENVIRONMENTS (MICROTENSILE SPECIMENS)

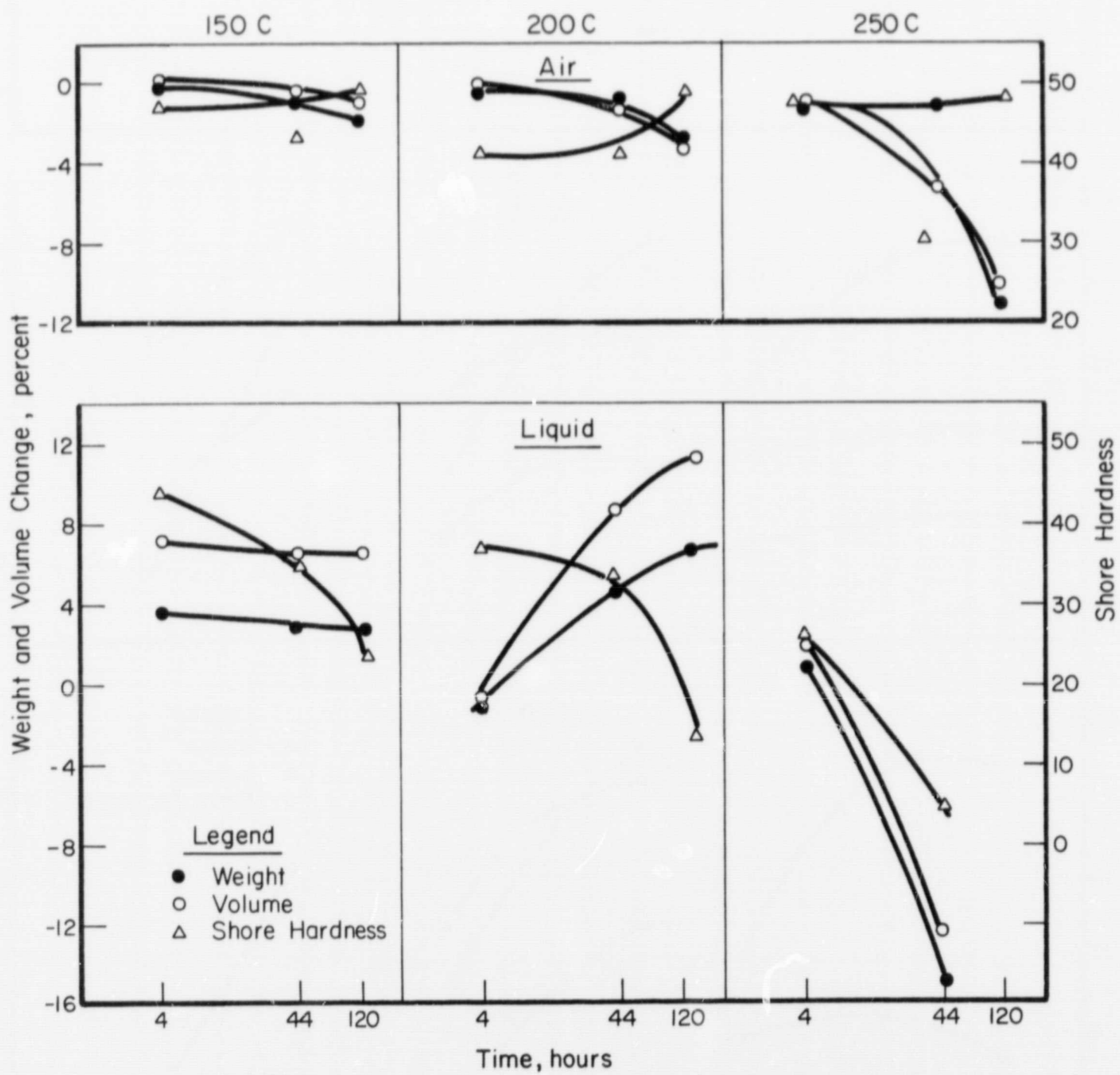


FIGURE 8. CHANGES IN WEIGHT, VOLUME, AND SHORE HARDNESS OF SEALANT 94-030 (LOT 911018) AS A FUNCTION OF TIME IN VARIOUS ENVIRONMENTS (DISK SPECIMENS)

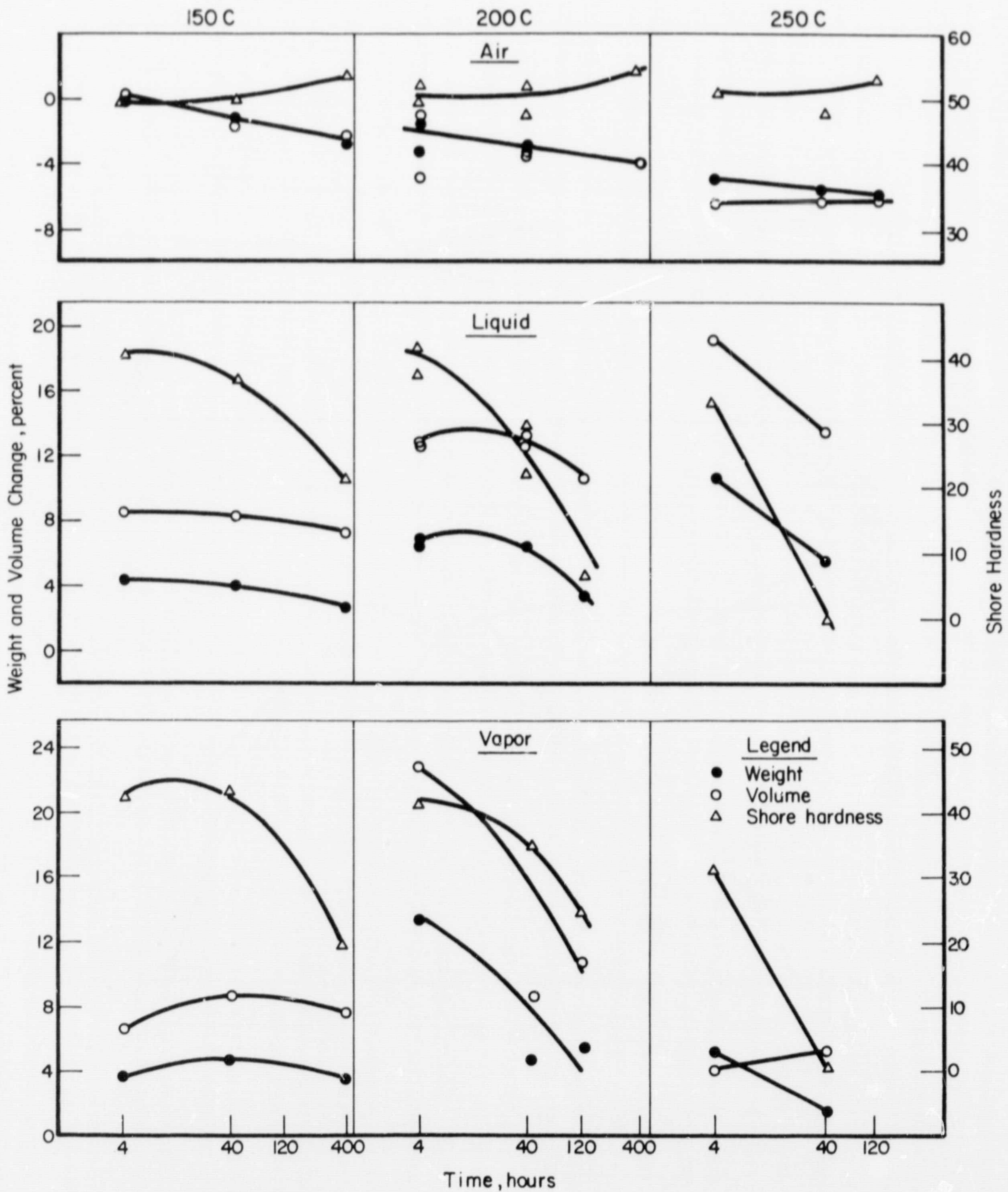


FIGURE 9. CHANGES IN WEIGHT, VOLUME, AND SHORE HARDNESS OF SEALANT 94-030 (LOT 911219) AS A FUNCTION OF TIME IN VARIOUS ENVIRONMENTS (MICROTENSILE SPECIMENS)

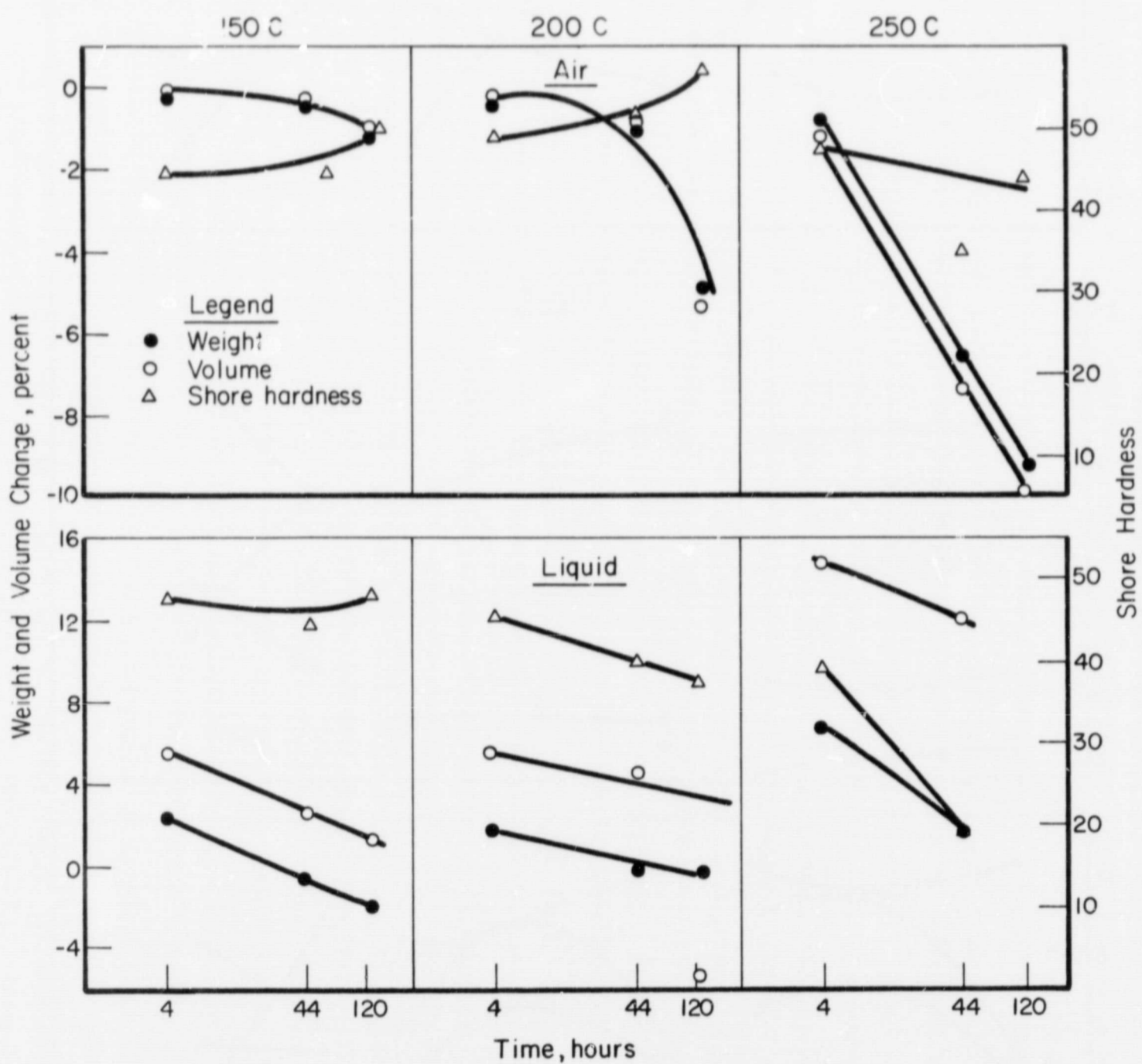


FIGURE 10. CHANGES IN WEIGHT, VOLUME, AND SHORE HARDNESS OF SEALANT 94-516 (LOT 901205) AS A FUNCTION OF TIME IN VARIOUS ENVIRONMENTS (DISK SPECIMENS)



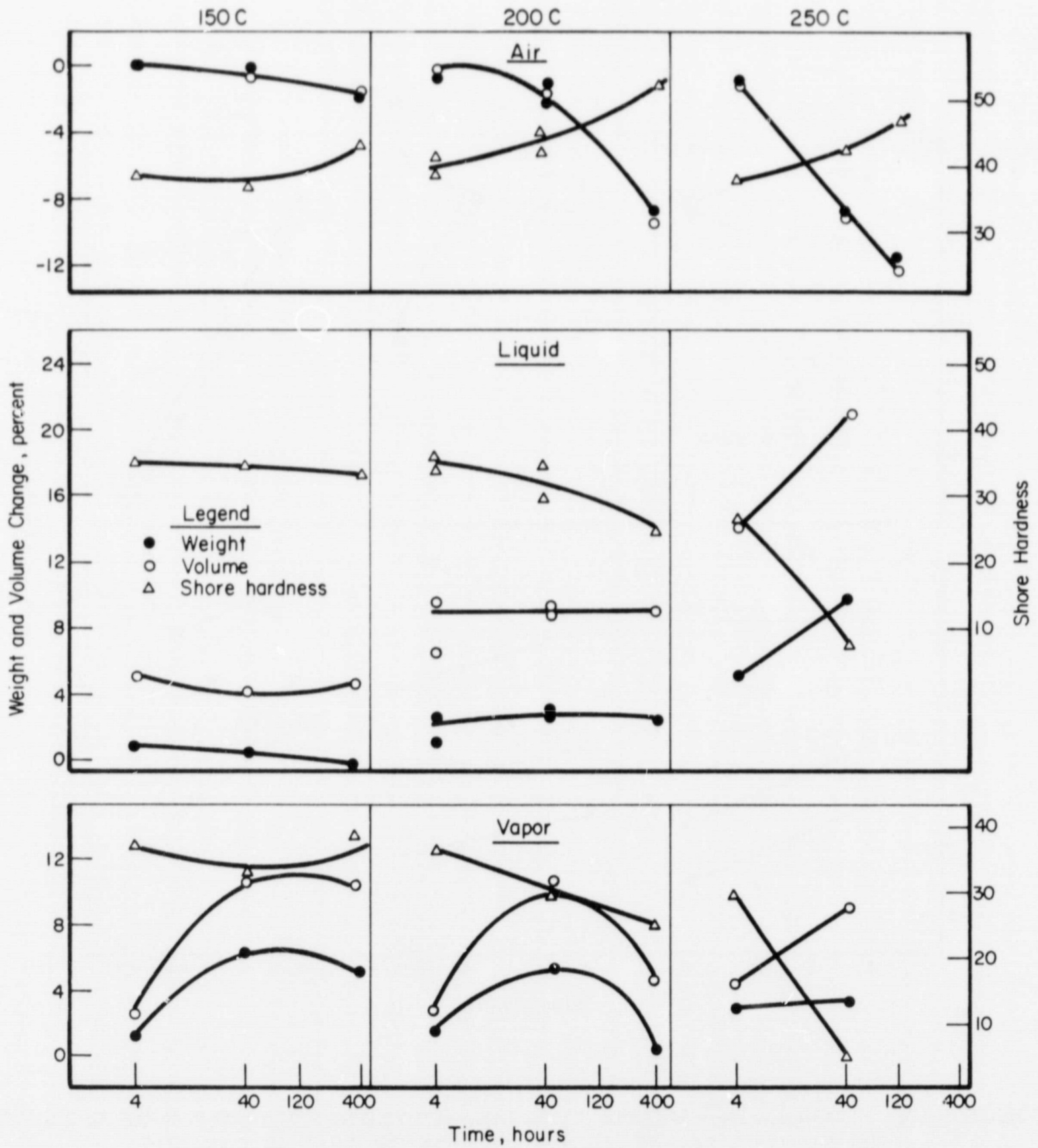


FIGURE 11. CHANGES IN WEIGHT, VOLUME, AND SHORE HARDNESS OF SEALANT 94-516 (LOT 002242) AS A FUNCTION OF TIME IN VARIOUS ENVIRONMENTS (MICROTENSILE SPECIMENS)

The much greater standard deviation of these measurements than was found in a round-robin test involving six laboratories<sup>(2)</sup> partially is a result of the stacking. Additional sources of error in Shore hardness measurements on aged specimens were observed with low-elongation and high-modulus specimens. The pressure probe cut through the low-elongation specimens, reducing the observed value. The aged specimens with high modulus usually had an uneven surface which did not flatten when the "foot" pressed on the specimen. This effect also reduces observed values.

Disk-shaped specimens of the sealants were used to estimate the precision of the weight and volume measurement. The specimens were first weighed in air, then in fuel, and blotted in a paper towel. This procedure was repeated five times. The initial weight and volume did not differ significantly from subsequent weights and volumes suggesting that there is no appreciable swelling at room temperature with these sealants and that the blotting technique is effective. Observed standard deviations were approximately 0.25 and 0.75 percent for the weight and volume, respectively.

#### Viton

The increase in rate of weight and volume loss of the Viton in air with increasing temperature indicates that the processes involved in these changes are temperature dependent as might be expected. The greater decrease in volume than in weight at 250 C and 120 hours suggests that, in addition to volatilization, the sample is shrinking. The marked decrease in rate of weight and volume loss with increasing time suggests that several simultaneous processes are initiated by heating the sample. In support of this suggestion is the change in Shore hardness with time of exposure of the Viton. It appears that during the first 4 hours, the predominating process results in a decrease in Shore hardness. A likely cause of this decrease is chain scission. However, it appears that a second process such as crosslinking predominates at longer exposures, which results in an increase in the sample's Shore hardness. The data suggest that the crosslinking reaction is strongly temperature dependent, while the initial process is only slightly temperature dependent.

It appears that several processes occur in fuel aging in addition to those observed during air aging. Apparently, swelling and extraction occur simultaneously. Initially, swelling is more rapid, as indicated by the weight increase of the sample. Since the observed weight includes absorbed solvent, the amount of material extracted from the sample is considerably more than that indicated by the weight loss. Therefore, it is clear that appreciably more material is extracted from the sealant when aged in fuel than is lost when heated in air. The initial decrease in Shore hardness for the fuel-aged specimens could be a result of a decrease in crosslink density brought about by the swelling. The rise in Shore hardness with continued aging exceeds the increase expected from the small volume decrease. Therefore, crosslinking reactions are undoubtedly occurring during aging in the fuel.

The initial swelling of this sealant is not likely to cause a fuel leak. However, the increase in Shore hardness with aging will result in higher stress on the sealant-substrate bond from seal deflections. The similarity of the changes in weight and volume resulting from exposure to fuel liquid or vapor indicates that a change in sealant environment from liquid to vapor will not cause appreciable desorption of fuel from the sealant.

(2) W. J. Mueller, private communication.

Dow Corning 94-030

As described previously, 94-030 is a single part, air-curing sealant. The by-product of the curing reaction is acetic acid, which must diffuse out of the sealant. Therefore, some of the initial losses in weight, when aged in air at the elevated temperature, may be due to loss of the acetic acid. The Shore hardness of both lots of this sealant goes through a minimum after exposure to air for approximately 44 hours and may indicate two processes of aging. The one which predominates before 44 hours is reduction in the crosslink density.\* The other which predominates at longer times is an increase in crosslink density caused by volatilization of low-molecular-weight products of aging and shrinkage. This sealant rapidly degrades in fuel, resulting in large reductions in the Shore hardness value, and at 250 C after 40 hours, the sealant has degraded to the point where it crumbles when stressed. The large losses in the Shore hardness accompanied with losses in both weight and volume indicate that the sealant is degrading by rupture of crosslinks or breakdown of polymer chains. The shorter chains produced by these reactions leach out of the sealant and the strength drops to essentially zero. Obviously, this sealant would provide a seal for only less than 40 hours in a fuel tank under these high-temperature conditions.

Dow Corning 94-516

Dow Corning 94-516 is a two-part, room-temperature curing system. Its behavior is similar to that of 94-030, except that it is more resistant to fuel below 250 C. At 250 C, the behavior of the two sealants is quite similar, showing a large reduction in Shore hardness. The 94-516 sealant becomes very soft from the exposure.

Over extended periods of time, the sealant begins to shrink, indicating extraction by the fuel, and the Shore hardness decreases, indicating a breakdown of the polymer network. This sealant, like 94-030, would very likely fail owing to channeling. The amount of fuel interaction for Viton, 94-030, and 94-516 sealants at all temperatures is about the same for the liquid as for the vapor, and during flight conditions, a significant amount of fuel would not be expected to desorb from the sealant as the temperature increases and the environment changes from liquid fuel to vapor. Dow Corning 94-516 too would not last more than 40 hours under actual flight conditions.

Tensile and Stress Relaxation

The effects of aging on Young's modulus, rupture stress, and ultimate elongation of the sealants are illustrated in Figures 12, 14, and 16. The data presented in these figures are tabulated in the appendix (see Tables A-2, A-4, and A-6). The effects of aging on stress relaxation are illustrated by examination of the modulus at 0.05 minute and the slope of the log-log plot of modulus versus time. The observed dependence of these properties on environments and time of exposure are illustrated in Figures 13, 15, and 17. The data used to construct these figures are presented in Appendix A (see Tables A-3, A-5, and A-7).

\*Crosslink density is the number of crosslinks per unit volume.

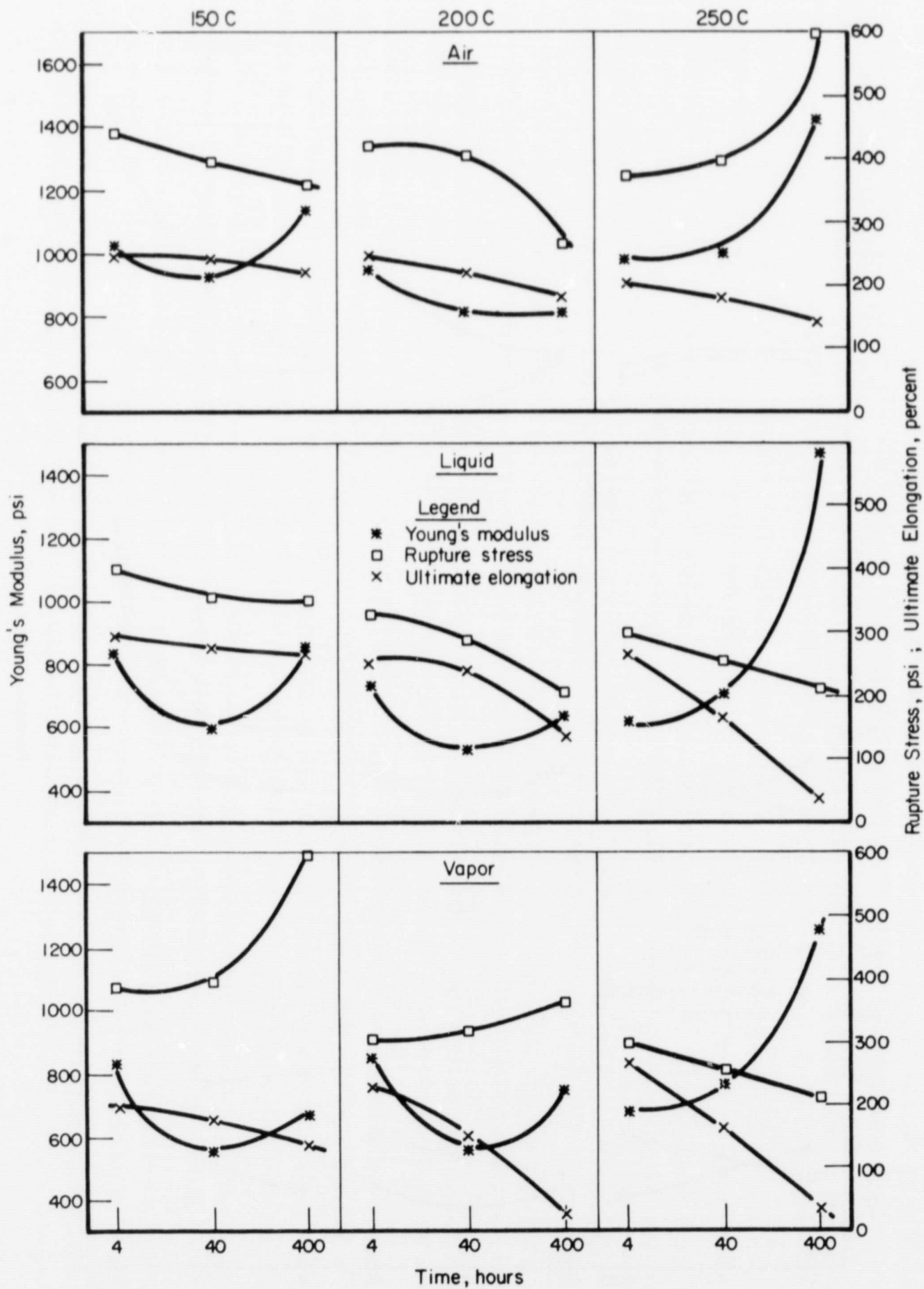


FIGURE 12. CHANGES IN TENSILE PROPERTIES OF THE VITON SEALANT AGED IN VARIOUS ENVIRONMENTS

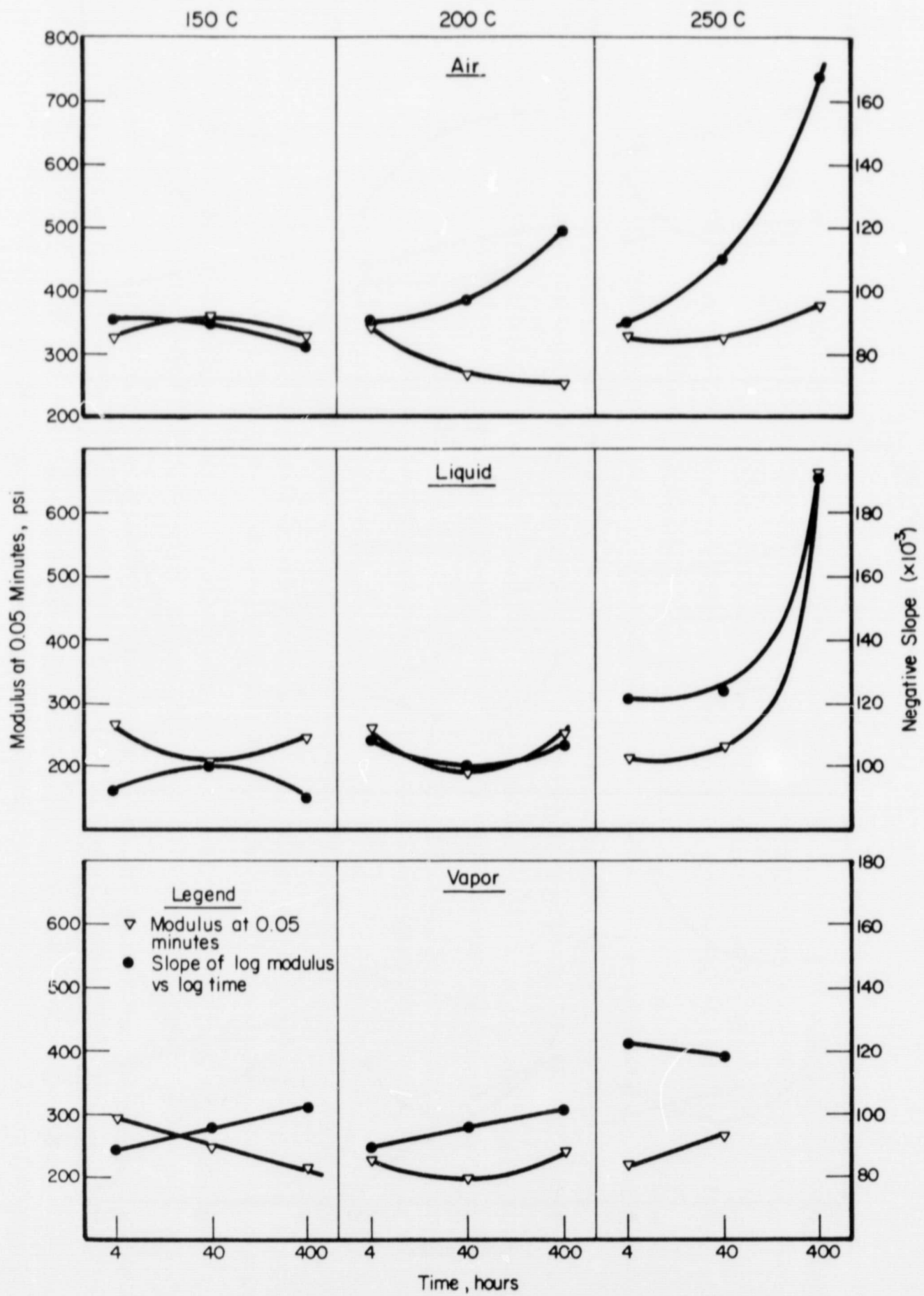


FIGURE 13. CHANGES IN THE STRESS-RELAXATION PROPERTIES OF VITON SEALANT AGED IN VARIOUS ENVIRONMENTS

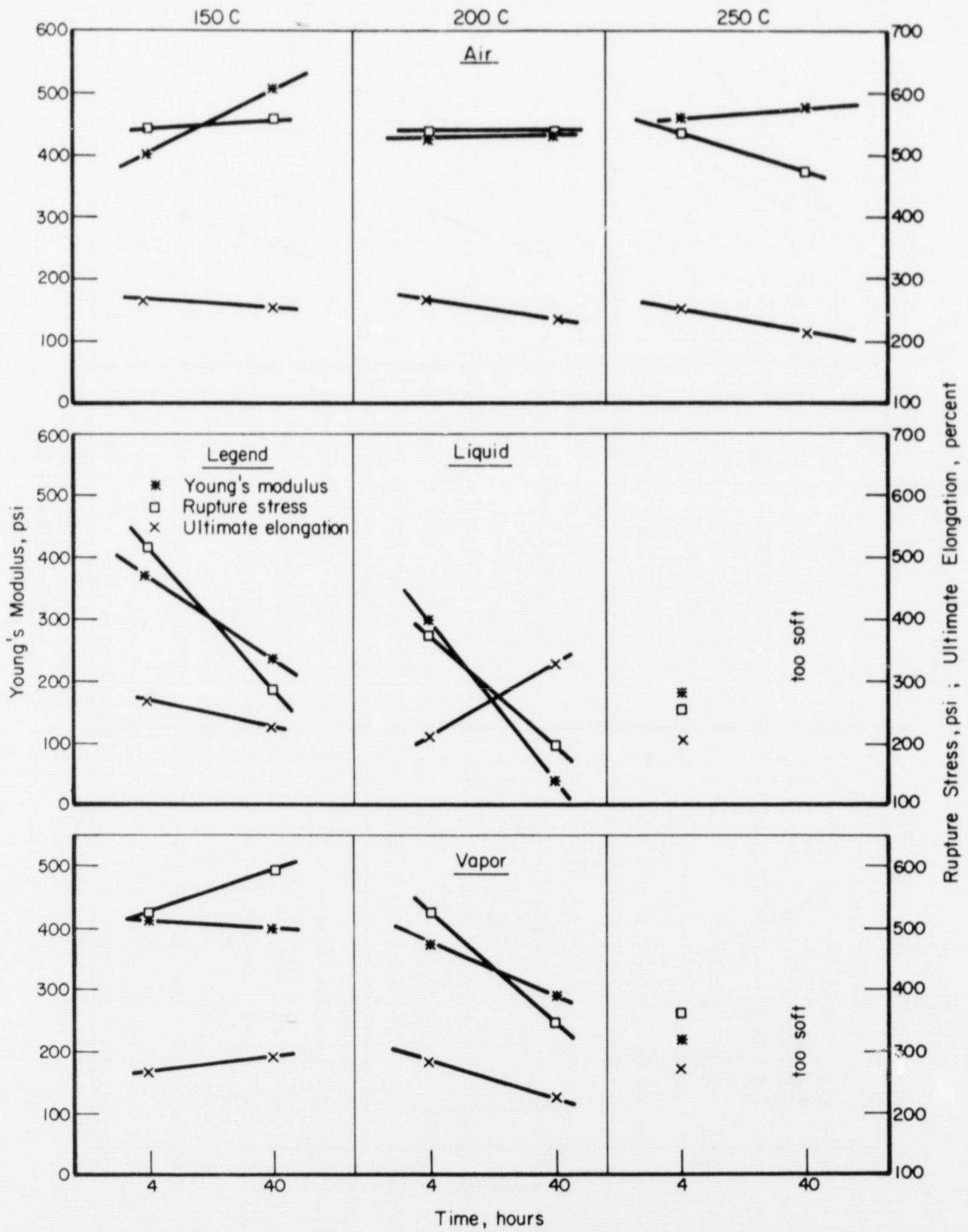


FIGURE 14. CHANGES IN THE TENSILE PROPERTIES OF THE DOW CORNING 94-030 SEALANT AGED IN VARIOUS ENVIRONMENTS

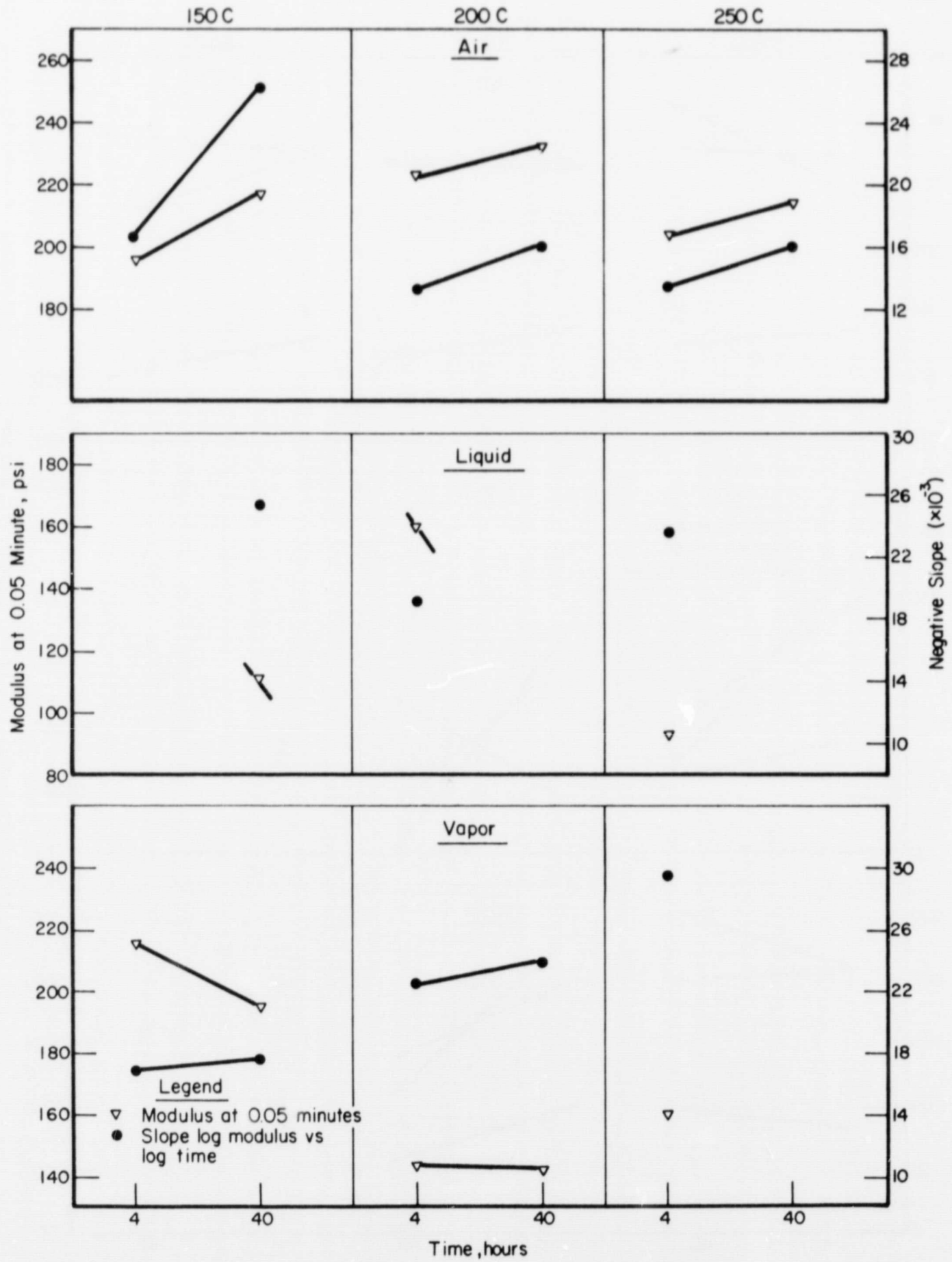


FIGURE 15. CHANGES IN STRESS-RELAXATION PROPERTIES OF DOW CORNING 94-030 SEALANT AGED IN VARIOUS ENVIRONMENTS

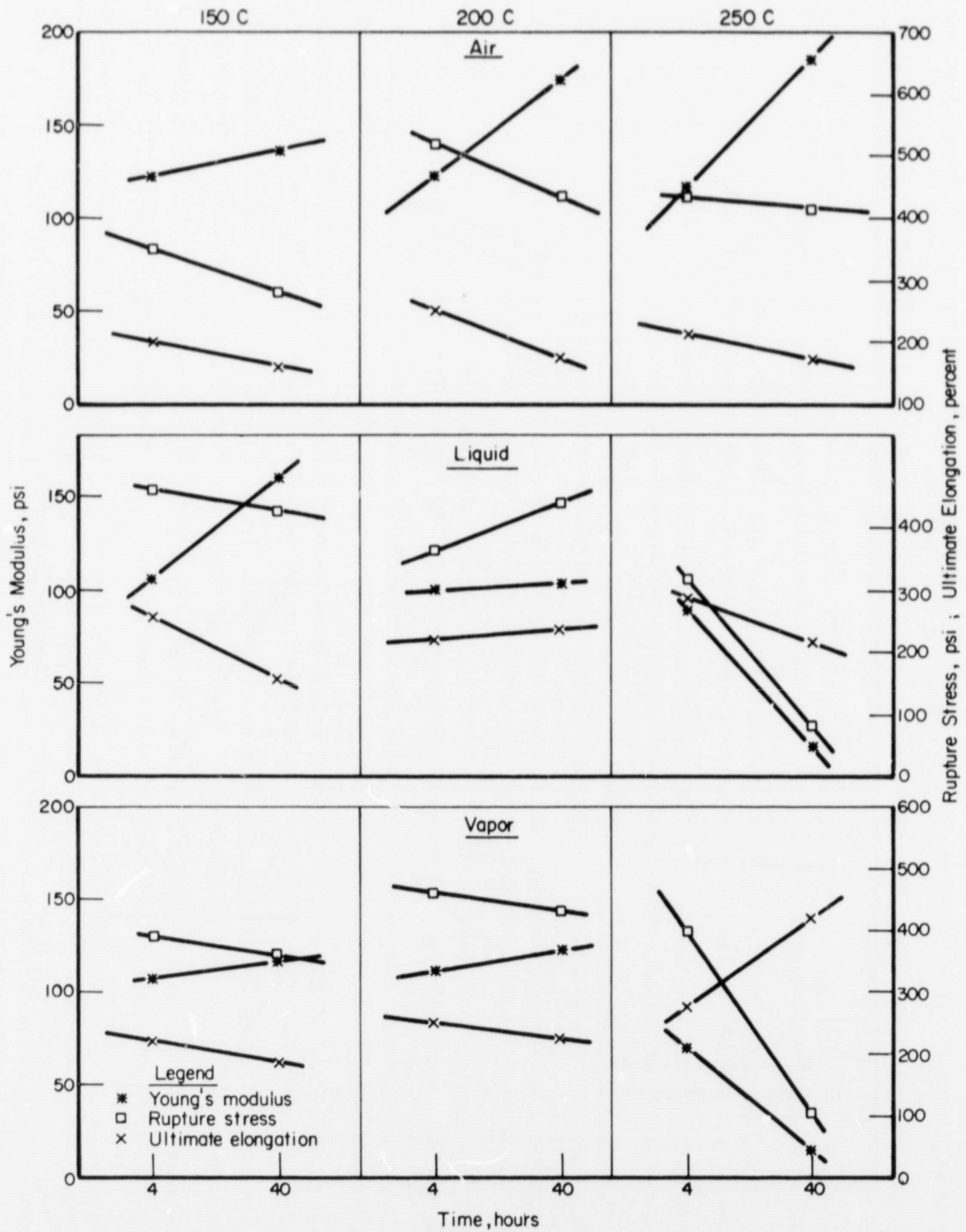


FIGURE 16. CHANGES IN TENSILE PROPERTIES OF THE DOW CORNING 94-516 SEALANT AGED IN VARIOUS ENVIRONMENTS



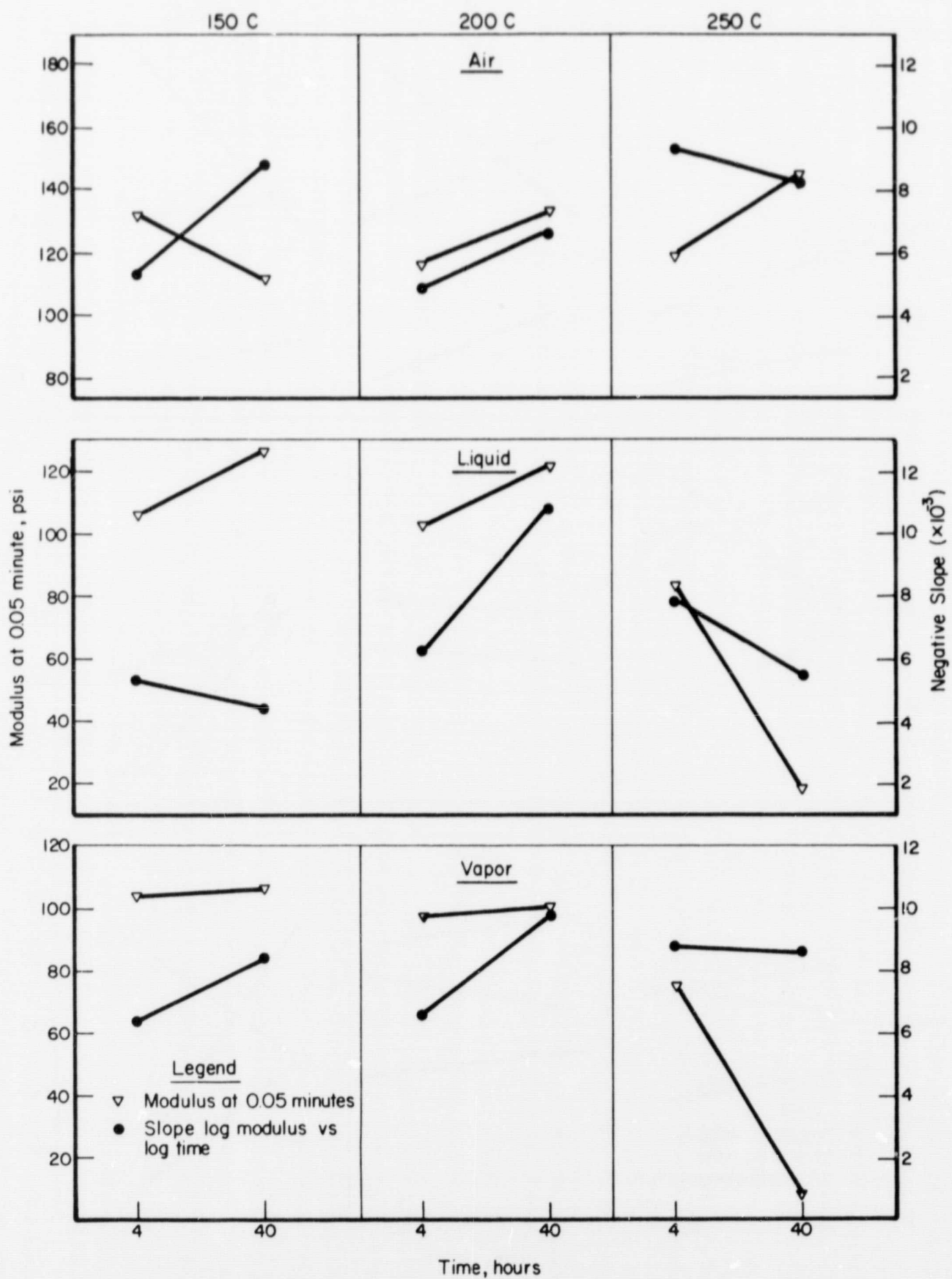


FIGURE 17. CHANGES IN STRESS-RELAXATION PROPERTIES OF DOW CORNING 94-516 SEALANT AGED IN VARIOUS ENVIRONMENTS

Viton

The tensile stress-strain curve of the Viton sealant differs from those observed for the other sealants and that expected for amorphous elastomeric materials. The curves, e.g., Figure 18, are characterized by a high initial slope, an intermediate shoulder, and a long linear region at high strain. The stress-strain curve is similar to that obtained with highly crystalline polymers such as high-density polyethylene. For these materials, the linear region at high stress is associated with irreversible deformation. The shape of the stress-strain curve suggests that two deformation mechanisms are operative, the high modulus region at low strain arising from Hookian (or spring) behavior of the polymer chains, while the linear region at high strain reflects viscous flow. The shoulder in the stress-strain curve probably corresponds to the onset of breakdown of crosslinks or polymer-filler bonds.

If polymer-filler bonds break down from stress, the sealant would interact more strongly with fuel than would the unstressed material. In this case, the effect of aging would depend on the stress on the material.

The modulus at 0.05 minute determined from the stress-relaxation measurement and the initial modulus or Young's modulus behave similarly. Young's modulus is larger than the 0.05 minute modulus by a factor of about three because this sealant has a high relaxation. This relaxation becomes important when considering deformations of low strain rates and slow temperature changes. Under these conditions, the stresses would have a chance to relax, and the forces exerted on the sealant substrate surface would be much less than that which would occur at high strain rates.

For all nine aging conditions, the ultimate elongation is reduced by aging. However, the effects of aging on rupture stress depends on the aging temperature and environment. For example, air aging at 150 and 200 C reduces the rupture stress with time, while aging at 250 C increases the rupture stress. In liquid, the rupture stress parallels the ultimate elongation; in vapor the rupture stress at the lower temperature increases and that at the high temperature decreases, even though the interaction between sealant and liquid fuel vapor is about the same at the lower temperature. For liquid at 250 C, and possibly vapor, Young's modulus, the 0.05-minute modulus, and slope or decay of the stress relaxation all increase. This indicates that the mechanisms which lead to rupture of the sealant are not paralleling those that affect the rheological properties measured at the lower elongations. Thus, in this case, failures due to adhesive loss caused by high stresses imposed by the high modulus would differ from failures due to cohesion, which is related to the ultimate elongation. The large increase in the relaxation slope at 400 hours and 250 C is very likely due to slippage and rupture of primary bonds during the measurement. The high Young's modulus supports this postulate, indicating a high crosslink density.

The minimum in Young's modulus as a function of time indicates two competing aging mechanisms. First, breakdown of primary bonds, and second, formation of crosslinks with consequent brittleness. The behavior of the Young's modulus of Viton when aged at 250 C is essentially independent of whether it was aged in liquid or vapor. However, at 150 and 200 C, the elongation is lower and the stress higher for those aged in vapor. This suggests that vapor aging is more severe than liquid aging below 250 C. The large Young's modulus coupled with large relaxation indicates that the stresses exerted on the adhesive bond would be much larger at high deformation rates than at low deformation rates.

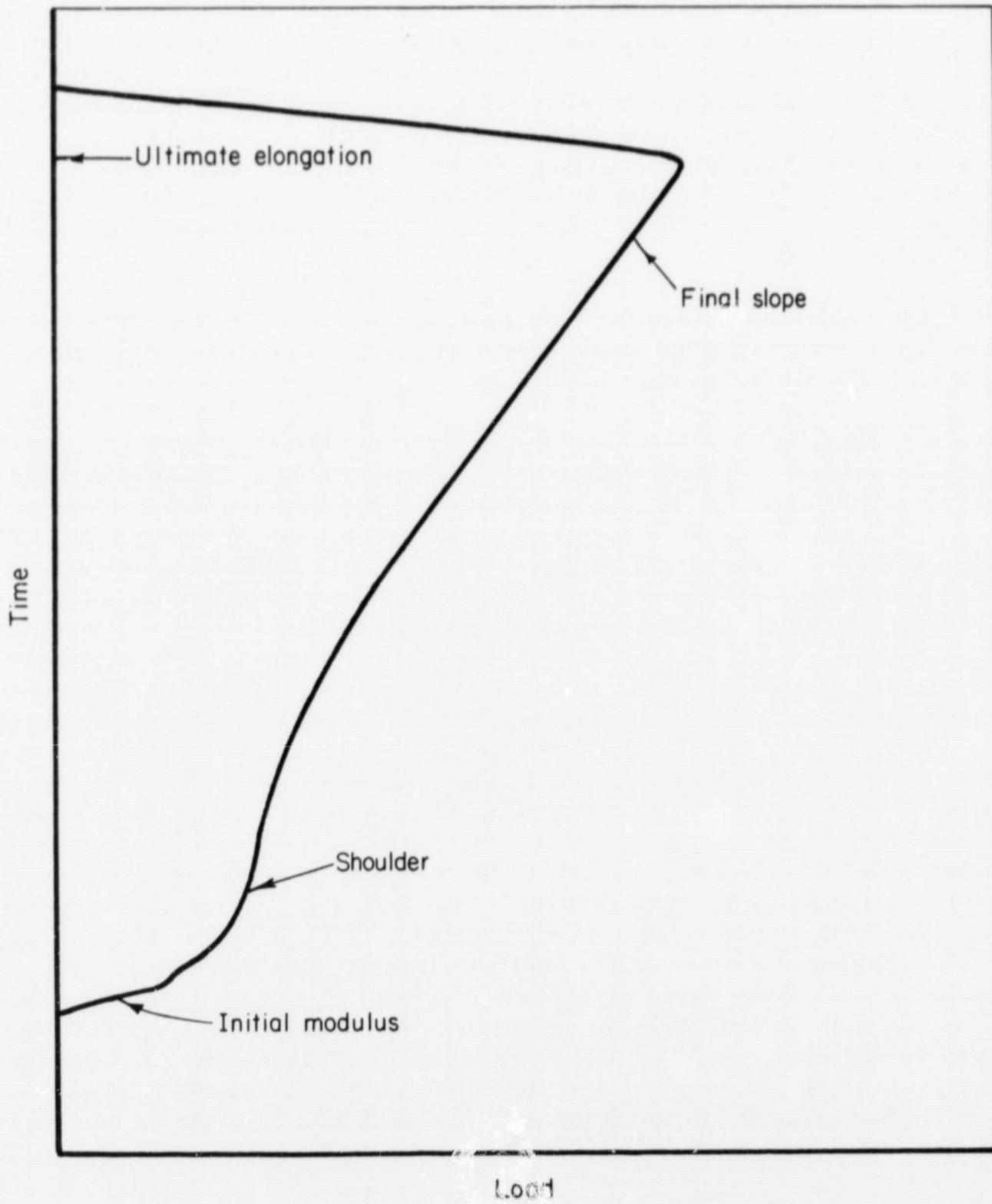


FIGURE 18. TYPICAL TENSILE LOAD-TIME CURVE FOR VITON SEALANT

The high relaxation slope in both the aged and unaged conditions indicates that this sealant has a large loss or viscous component. Therefore, high deformation rates would produce viscous heating and temperatures in the sealant would be higher than the surrounding environment. This would reduce the stresses throughout the sealant but decrease the sealant's service life.

#### Dow Corning 94-030

The changes in stress relaxation and tensile properties for Dow Corning 94-030 caused by aging are shown in Figures 14 and 15. This sealant degraded so rapidly in fuel at elevated temperatures that neither tensile values for 40 hours at 250 C nor stress relaxation at 40 hours at 200 C could be obtained.

The tensile load-time curve for this sealant was typical of elastomeric materials, i. e., the initial slope was slightly larger than the final slope. Young's modulus and the modulus at 0.05 minute in the stress-relaxation test behave similarly with Young's modulus being about twice as large.

This sealant has a much lower relaxation than Viton (about one-fifth). Also, the ultimate elongation does not decrease as rapidly and to the same extent as that of Viton. The decrease in Young's modulus and rupture strength indicates rapid degradation at high temperatures in fuel, but this is not reflected in the elongation. This sealant most likely degrades by rupture of primary bonds, permitting swelling and extraction. The large drop in both weight and volume at 120 hours and 200 C supports this view (see Figure 9). At higher temperatures, this sealant would act essentially like a viscous fluid, while it would undoubtedly behave like a low-strength, brittle solid at lower temperatures. This sealant interacts strongly with fuel, becomes soft, and swells to a great extent. Therefore, it will fail cohesively unless the adhesive strength also decreases with aging, in which case both adhesive and cohesive failure can occur.

#### Dow Corning 94-516

The effects of aging on tensile and stress-relaxation properties of 94-516 sealant are illustrated in Figures 16 and 17. Degradation is rapid, but not to the extent of that of 94-030. Stress relaxation, as determined by the slope, is about one-half that of 94-030, and one-tenth that of Viton. Therefore, the stresses will not decay as rapidly. The Young's modulus and stress-relaxation modulus at 0.05 minute are very similar in behavior, and the magnitude of the two are about equal.\* In this sealant, elongation is increased by fuel interaction. However, at the elevated temperature, the rupture stress is decreased significantly as is Young's modulus. This most likely is caused by a breakdown of primary polymer bonds, leading to the increased swelling demonstrated by the volume increase shown in Figure 11. Adhesive failures are unlikely at low stress, unless the adhesive bond also degrades.

This sealant would most likely work best in the faying seal. If used in a filleting seal, its lower Young's modulus and rupture stress would lead to failure from stresses exerted by fuel motion around the sealant. In this sealant, as with 94-030, the ultimate

---

\*The difference between Young's modulus and the 0.05-minute modulus from stress relaxation depends on the stress-relaxation slope, i. e., the smaller the slope, the smaller the difference.

elongation is high at the measured strain rates. However, the low Young's modulus of the aged specimen indicates that they have a low crosslink density. Therefore, the ultimate elongation of aged materials at lower strain rates would be expected to be substantially less.

### Torsional Damping

Determination of the torsional damping of disk specimens with the Weissenberg Rheogoniometer was found to be complicated by some unforeseen problems. The only expected complication was from effects of compressive loads on the specimen when placed between the platens of the Rheogoniometer (some compressive load is needed to obtain a nonslip contact between the platens and the specimen). Initially, this effect was thought to be minimized by compressing the specimens to 98.5 percent of their unstressed height. However, the surfaces of the aged disks were not flat or parallel and this prevented accurate identification of dimensions for compression. This influenced the behavior of the specimen by exerting uneven compressive loads throughout the disk.

These factors affect the damping properties of the sealants so that the decrement and the frequency values obtained are a function of not only the material properties of the sealant, but also the geometry. Figure 19 illustrates the effect of compressive stress on the natural frequency during torsional damping. It is obvious that the frequency is affected most at lower stresses.

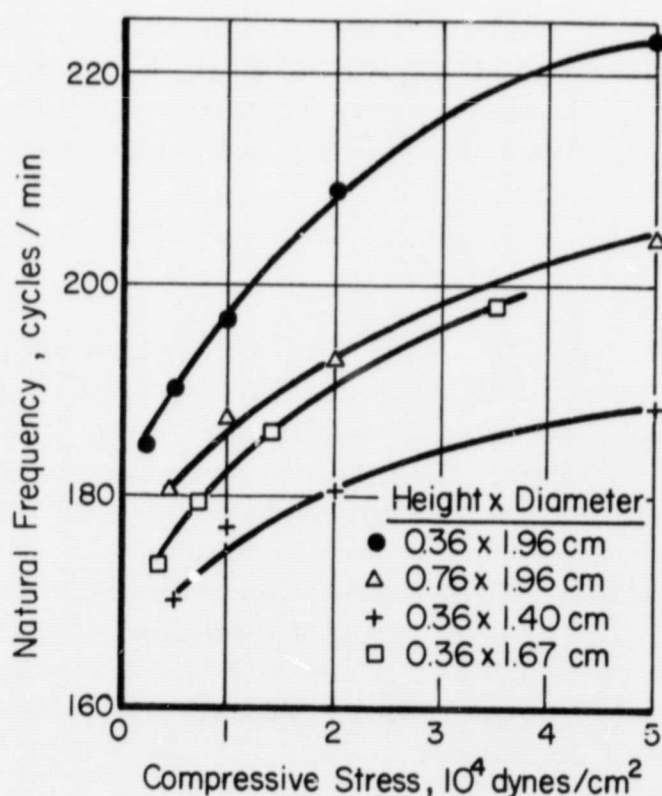


FIGURE 19. EFFECT OF COMPRESSIVE STRESS ON THE NATURAL FREQUENCY DURING TORSIONAL DAMPING

A rheological model is required to convert the data from frequency and decrement to a material property such as a modulus. For these materials, a Voigt model was assumed. Viscous and an elastic moduli were calculated using the equation derived in Appendix B. However, the geometric factor in the literature<sup>(3,4)</sup> is given as  $\pi R^4/2H$ , where R is the radius and H is the height. This factor does not appear to be of the correct form. Calculations of this factor from the data shown in Figure 19, using the equation shown in the Appendix B gives

$$\pi R^{2.6} / 2H^{0.5} .$$

These calculated exponents are not independent of the compressive load, but become larger as the compressive load decreases. Consequently, the moduli calculated using the Voigt model and this geometric factor are questionable.

The error in the calculated moduli introduced by changes in the real moduli will be opposite to that for the Shore hardness measurement. As the modulus increases, the compressive load at 1.5 percent compression will become larger, causing a higher frequency, which then leads to overall larger moduli.

Some of these problems could have been avoided by using a specimen of a different geometry, such as a tensile specimen. Specimens of this shape can be clamped without exerting large compressive effects. However, the tensile specimen also is sensitive to tensile or compressive loads, but probably to a lesser degree, as indicated by the smaller-diameter specimen in Figure 19. With a tensile specimen, the force exerted on the torsional equipment by viscoelastic material is much smaller than that with a disk. Consequently, slight air currents will cause gross irregularities in the motion of a torsional system such as the rheogoniometer, and equipment of a different design must be used.

These complications on the measured torsional-damping properties of disks exaggerate the real changes in the moduli; that is, if the modulus increases, then the compressive stress at a constant deformation would be larger, thus increasing the frequency which leads to a still larger calculated modulus. If the modulus decreases, the compressive stress at a constant deformation is less, and the frequency would be increased less, thus producing too low a relative calculated modulus change. However, if the geometry changes irregularly, then the calculated moduli could either be too small or too large, depending on the way in which the geometry changes.

Despite these complications, informative data can be obtained on viscoelastic sealants by this method. Some examples of such data are shown in Figures 20 and 21, where the effect of cure at room temperature on the torsional damping of two lots of the 94-516 sealant are shown. These measurements were not influenced by the complications discussed above because the uncured sealant was cast between the platens and allowed to cure without removing it. Thus, compressive stresses were not present because the geometry of the specimens was the same as that of the platens. The effect of cure on the natural frequency of the sample using the three inertial positions is shown in Figure 20. Again, using the Voigt model for analysis of the torsional damping measurement, the complex moduli were determined and are shown in Figure 21. The difference in Shore hardness of these two sealant lots shown in Table 3 is consistent with the difference in curing behavior observed by torsional damping.

(3) Ferry, J. D., *Viscoelastic Properties of Polymers*, Wiley and Sons, Inc., New York (1961), p 119.

(4) *The Weissenberg Rheogoniometer*, Instruction Manual Model R. 18, Sangamo Controls Ltd., Sussex England, Section D.

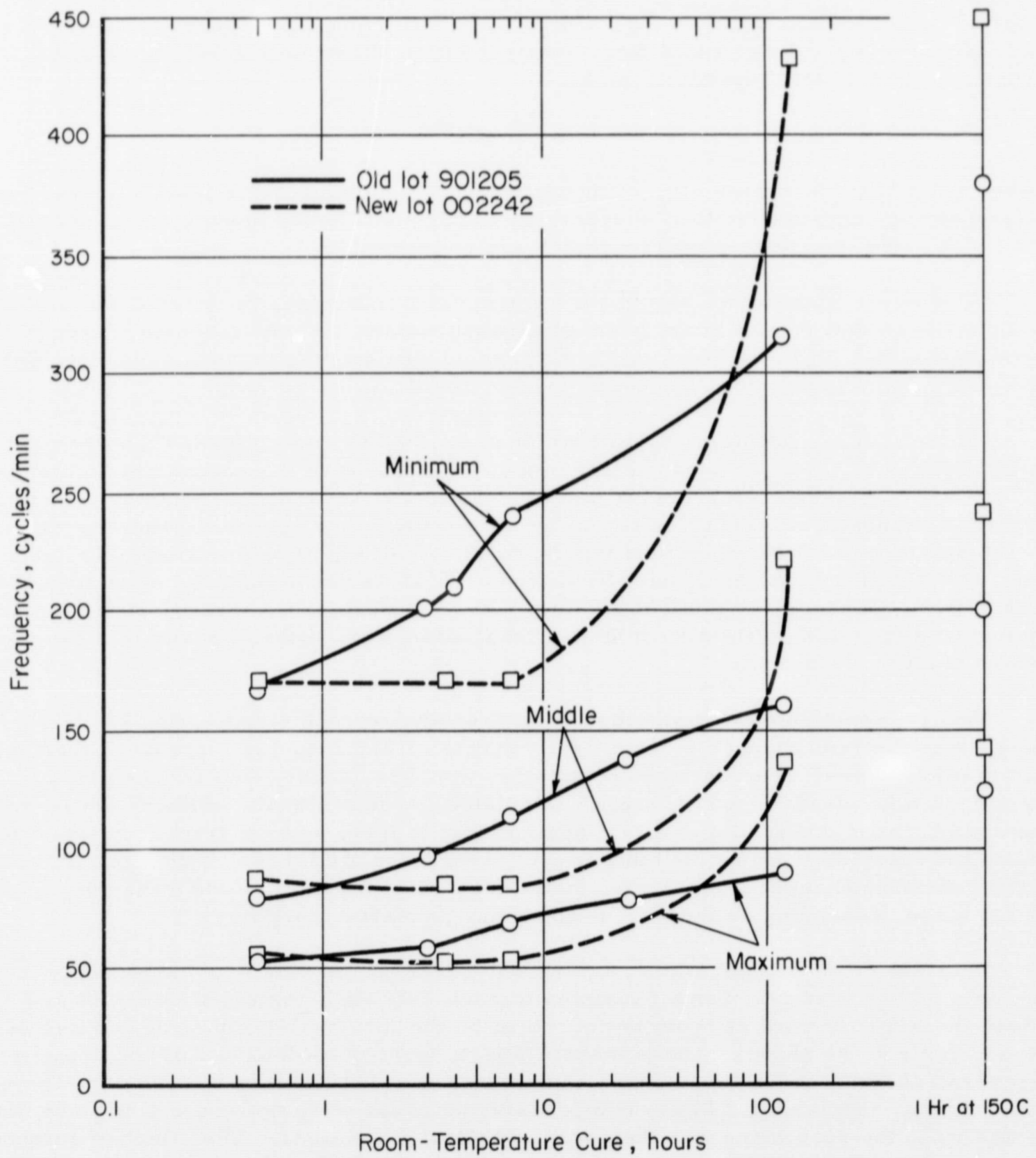


FIGURE 20. EFFECT OF CURE ON THE TORSIONAL DAMPING FREQUENCY OF SEALANT 94-516

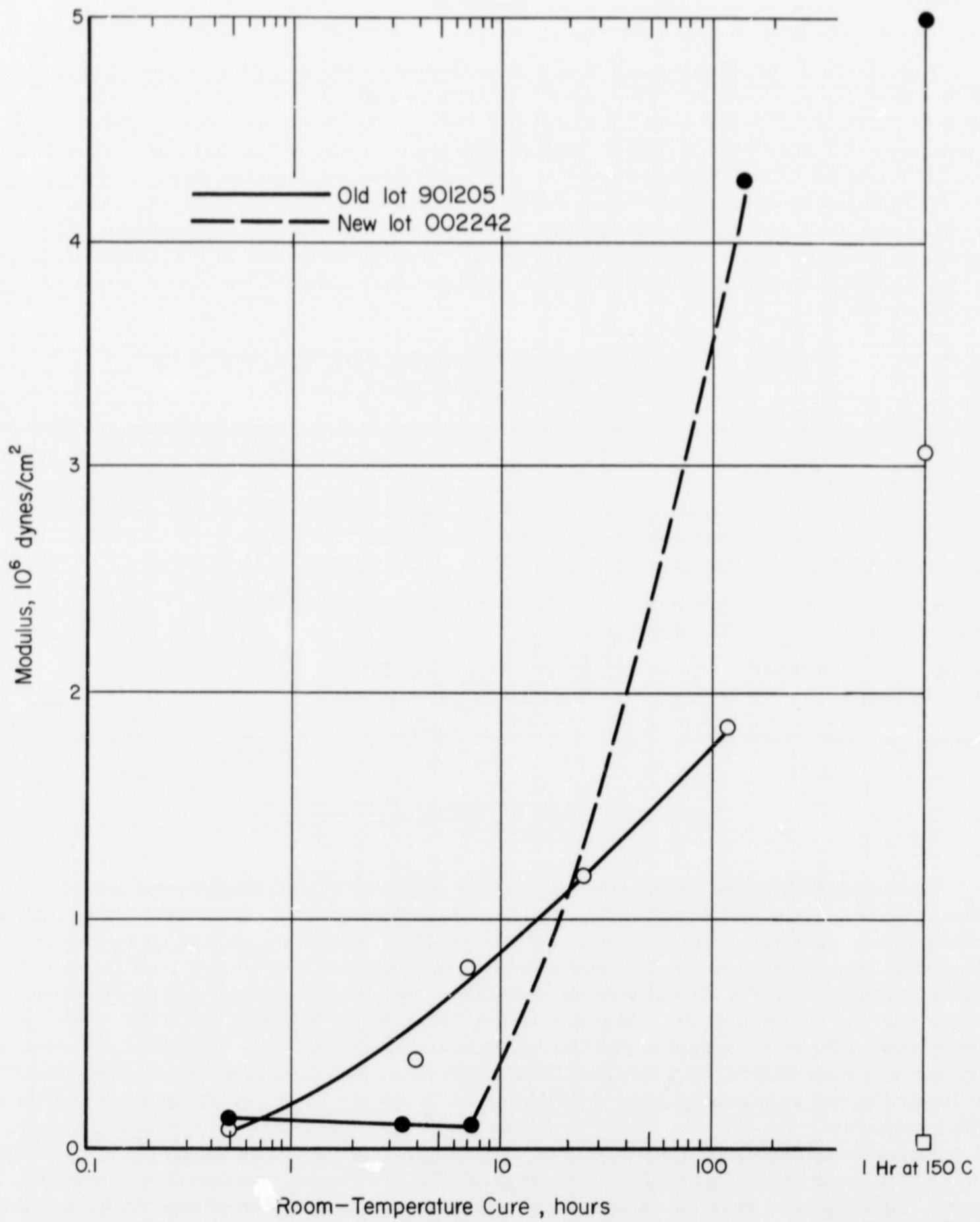


FIGURE 21. EFFECT OF CURE ON THE TORSIONAL DAMPING COMPLEX MODULUS OF SEALANT 94-516



Adhesion

The adhesive properties of the two Dow Corning sealants were investigated using single lap shear specimens. The results of tensile tests on some unaged specimens are shown in Table 4. The standard deviation of the lap shear stress was approximately 30 percent. Because of difficulties with preparation of uniform specimens, no conclusions about aging of the adhesive bond could be obtained during this period. Discussion of the large standard deviation with a representative from Dow Corning revealed that the lap shear specimens should be prepared in ultraclean conditions. Otherwise, large variations in the lap shear strength will occur. Rather than construct a special room for these preparations, a glove box with a constant humidity (50 to 70 percent) could serve as well.

TABLE 4. INITIAL MEASUREMENTS OF SEALANTS IN SINGLE LAP SHEAR ON Ti-6Al-4V

Sealant	Primer	Cure	Stress, psi	Deviation	No. of Specimens
94-516 (Lot-002242)	77-006	Primer: 16 hr at 60 percent RH Sealant: 1 hr, 150 C	130	53	5
94-516 (Lot-002242)	77-006	Primer: 1-1/2 hr at 60 percent RH Sealant: 1 hr, 150 C	229	80	10
94-030 (Lot-911018)	92-040	Primer: 16 hr at 60 percent RH Sealant: 17 days at 60 percent RH	284	114	5

Factors Related to Sealant Performance

In the preceding sections, measurements of physical and rheological properties of the three sealants were reported. These measurements have provided some insight into the associated aging phenomena. In this section, relations will be derived for estimating stress and elongation requirements of sealants in two joint configurations in order to relate property changes to service life. Strains on the sealant arise from volume changes in the sealant, changes in the relative positions of the substrates, or differences in thermal expansion of the substrate and the sealant. Although all sources of strain are expected to be operative during service, the significance of each source will be evaluated separately. One configuration, a faying joint, is illustrated in Figure 22. In this configuration, the sealant is confined between overlapping metal substrates which are separated by approximately 0.001 to 0.010 inch. A second configuration, the fillet joint, is illustrated in Figure 24. The edge of the overlap of two metal substrates is shown. Clearly, the strains on sealants in the two configurations produced by movement of the substrates are quite different. Therefore, the two joint configurations also will be considered separately.

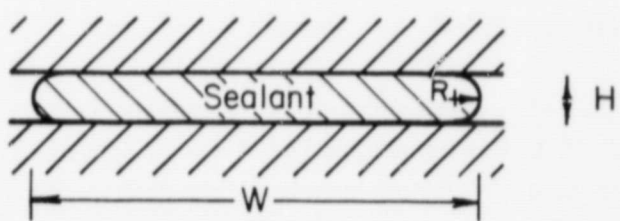


FIGURE 22. FAYING CONFIGURATION

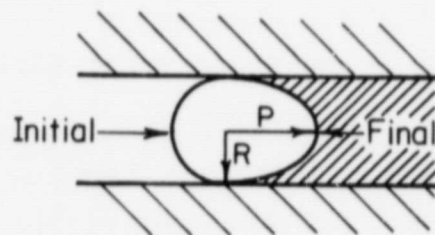


FIGURE 23. SURFACE OF THE SEALANT IN A FAYING CONFIGURATION BEFORE AND AFTER SHRINKING

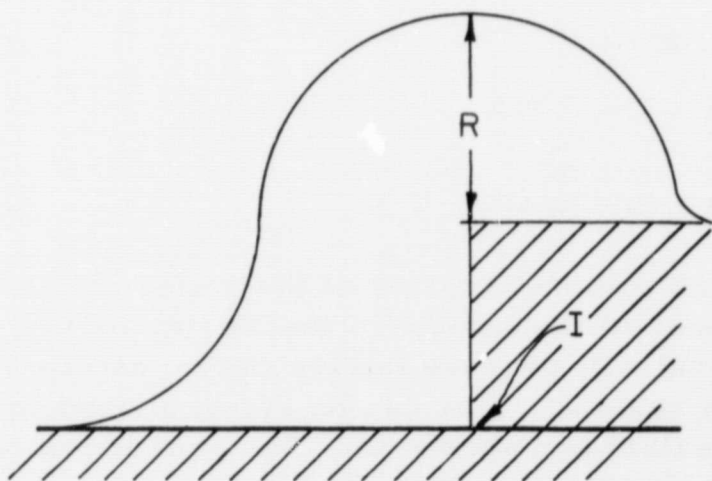


FIGURE 24. FILLETING CONFIGURATION

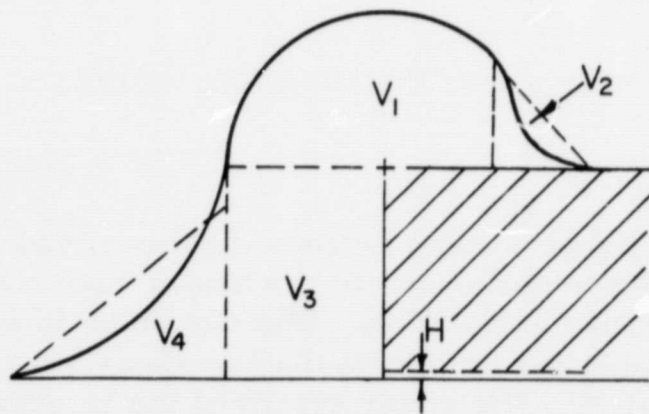


FIGURE 25. SEPARATION OF FILLETING SEAL INTO VOLUME ELEMENTS

### Volume Changes in the Faying Sealant

For analysis of the stresses produced by volume changes in a faying joint, it is assumed that: (1) the projection of the sealant surface generated by a volume change can be represented by a parabola, (2) the relative positions of the substrates do not change, (3) stress resulting from shrinking can be relieved only by changing sealant shape, i. e., no cohesive failure of the sealant, and (4) the maximum force on the sealant from volume changes will be on its surface. The volume of sealant in the faying surface joint is

$$V = WHL + \pi R^2 L = LH(W + \pi H/4) , \quad (1)$$

where  $W$  is the width,  $H$  is the height (separation of the substrates),  $L$  is the length of the sealant, and  $R$  is the radius of the semicircle at the sealant edge (see Figure 22).  $H$  is equal to  $2R$ . The semicircle is created when the uncured sealant is compressed between the substrates.

The change in volume of the sealant (see Figure 23) is the difference between the volume enclosed by the parabolic surface, i. e.,

$$V = 4/3 P (H/2) L , \quad (2)$$

and the volume enclosed by the semicircle. That is

$$\Delta V = L(4PH/3 \pm \pi H^2/4) = LH(4P/3 \pm \pi H/4) . \quad (3)$$

The plus sign applies to shrinking while the negative sign applies to swelling. Therefore, the fractional change in volume is

$$\Delta V/V = (4P/3 \pm \pi H/4) / (W \pm \pi H/4) . \quad (4)$$

To simplify, define

$$a = P/H \text{ and } b = W/H . \quad (5)$$

Substituting into Equation (4), we obtain

$$\Delta V/V = (4a/3 \pm \pi/4) / (b \pm \pi/4) . \quad (6)$$

This equation then defines the fractional change in volume in terms of the ratios of the parabolic deflection to the height, and the thickness of the sealant to the height, or faying substrate separation. The decrease in volume that will produce failure can be estimated from the magnitude of the lap shear strain of the sealant. This can be accomplished by calculating the shear strain at the interface of sealant and substrate. The equation of the projection of the surface is

$$y = (P/R^2) x^2 - P , \quad (7)$$

where  $x = y = 0$  at the centers of sealant-substrate contact points.

The shear strain at a sealant-substrate interface boundary is

$$\left| \frac{dy}{dx} \right|_{x=R} = 2P/R = 4P/H = 4a \quad (8)$$

The maximum stress that can be supported without adhesive rupture is

$$G \cdot 4/a = S \quad (9)$$

where  $G$  is the shear modulus and  $S$  is the lap shear strength. Substituting into the form of Equation (6) appropriate for shrinkage, we obtain

$$\Delta V/V = (S/3G + \pi/4) / (b + \pi/4) \quad (10)$$

The term  $b$  will be much greater than  $\pi/4$  in ordinary faying seals. Therefore, the denominator can be approximated by  $b$ . Since the shear modulus,  $G$ , for elastomeric materials is equal to  $1/3 E$ , the tensile or, more correctly, Young's modulus,

$$\Delta V/V = (S/E + \pi/4) / b \quad (11)$$

Thus, the volume decrease that will cause adhesive rupture is related to the ratio between the lap shear strength and Young's modulus.

When the sealant swells, adhesive rupture is not likely because a compressive force is exerted at the sealant-substrate interface. Therefore, the force required to rupture the adhesive bond must be extremely large. As the sealant expands, failure will most likely be due to, or at least initiated by, cohesive rupture. An indication of shrinking and swelling strains can be obtained from the equation for the length of a parabola, i.e.,

$$L_P = \sqrt{4P^2 + H^2} + \frac{H^2}{2P} \ln \left[ \frac{2P + \sqrt{4P^2 + H^2}}{H} \right] \quad (12)$$

Substituting the relations given in Equation (5) and Equation (12) yields

$$L_P = H \left[ \sqrt{4a^2 + 1} + (1/2a) \ln (2 + \sqrt{4a^2 + 1}) \right] \quad (13)$$

Since the sealant is not strained by shrinking until the volume is less than the rectangle included within the boundary of the sealant-substrate contact, the unstrained length is  $H$ . Therefore, the surface strain from shrinking,  $\epsilon_{sh}$ , is

$$\epsilon_{sh} = \frac{L_P - H}{H} = \frac{L_P}{H} - 1 \quad (14)$$

Conversely, the surface strain from swelling,  $\epsilon_{sw}$ , is

$$\epsilon_{sw} = \frac{L_P - \frac{\pi H}{2}}{\frac{\pi H}{2}} = \frac{2L_P}{\pi H} - 1 \quad (15)$$

Equation (6) was used to obtain values of  $a$  associated with volume changes of the sealant for specified seal dimensions, i.e., values of  $b$ . Substituting the values of  $a$  so obtained into Equation (13) leads to an associated  $L_p$ . The tensile strain for shrinking or swelling can be obtained by substituting the value of  $L_p$  into Equation (14) or (15), respectively. The results of these calculations are given in Table 5. Since tensile strains in excess of the sealant's maximum are predicted, it appears that surface cracking is likely. However, introduction of a crack would not result in failure unless the crack were propagated through the sealant. Therefore, the force necessary to propagate a crack is a natural property which must be measured in order to predict failure. Since the force necessary to propagate a crack in the candidate sealants investigated in this program, particularly those obtained from Dow Corning, was considerably less than their rupture stress, surface rupture induced by volume changes is a likely failure mechanism.

TABLE 5. TENSILE STRAINS PRODUCED BY VOLUME CHANGES IN FAYING SEALANT

Volume Change, percent	Tensile Strain		b
	Shrinking	Swelling	
8	0.006	0.218	10
10	0.14	0.50	10
13	0.49	0.92	10
15	0.80	1.20	10
20	1.33	1.86	10
25	2.76	2.74	10
30	3.88	3.52	10
3	0.80	1.22	50
5	2.76	2.74	50
8	6.26	3.16	50
10	8.76	6.84	50
1	0.14	0.50	100
3	3.90	3.52	100
5	8.76	6.84	100
7	14.04	12.32	100

#### Volume Changes in the Filleting Sealant

For analysis of the stresses resulting from volume changes of the sealant on a fillet seal, it was assumed that the sections defined by the dashed lines in Figures 24 and 25 provide a reasonable approximation to the cross-sectional areas of a fillet seal before and after shrinking, respectively. The initial volume of the seal,  $V_0$ , is then

$$V_0 = \left( \frac{\pi R^2}{2} + R^2 + 1/3 R^2 \right) L, \quad (16)$$

where  $L$  is the length of the joint. The volume of the sealant after shrinking is approximately

$$V = \left[ \frac{\pi(R^1)^2}{2} + 1/3 R^1 (R - R^1) + RR^1 + 1/3 R (2R - R^1) \right] L . \quad (17)$$

Assuming  $R^1$  is some fraction,  $c$ , of  $R$  and rearranging one obtains

$$V = R^2 [c^2 (\pi/2 - 1/3) + c + 2/3] L . \quad (18)$$

Therefore, the fractional volume change is

$$\frac{\Delta V}{V} = (2.237 - 1.237 c^2 - c) / 2.904 . \quad (19)$$

Although the volume elements shown in Figure 25 are shown on sealant in a fillet joint which has shrunk, they also provide a reasonable approximation to swollen sealant. A change in the length of the exposed edge of the sealant will produce strain in the sealant. Since this length depends directly on  $R$ , a change in  $R$  will produce a proportionate strain. Using Equation (19), it was found that a 10 percent change in  $R$  produces approximately a 34 percent volume change. Clearly, the volume of sealant in a fillet joint can change appreciably without producing critical strains.

#### Substrate Movements for Both Joint Configurations

The requirement placed on the sealant by movement of one substrate relative to the other is illustrated by examination of a movement of one substrate 45 degrees to the plane of the other substrate. Such a movement (or deflection) would have the same effect as two simultaneous deflections perpendicular and parallel to the substrate, respectively. If the 45-degree movement was for a distance  $d\sqrt{2}$ , then the new movement would be for a distance  $d$ . The deflection perpendicular to the substrate will produce a tensile strain equal to  $d/H$  ( $H$  is the substrate separation), and the deflection parallel to the substrate will produce a shear strain also equal to  $d/H$ . Obviously, increasing  $H$  will decrease the strain on the sealant. If the maximum deflection at the joint is 0.008 inch as specified by Boeing\*, then  $H$  must be greater than 0.004 inch to avoid rupture with the Dow Corning sealants after 40 hours and greater than 0.027 inch to avoid rupture with the Viton sealant after 400 hours in the most severe aging conditions.

The effect of rupture depends strongly on the seal configuration. In a faying joint, failure will result if sufficient strain to cause rupture is available. Conversely, strains of the same magnitude are present at Point I in Figure 24, but the possibility of failure is reduced because the strain imposed decreases in moving from Point I to the edge of the seal. If the length of the projection of the exposed edge of the seal can be approximated by  $5R$ , then for typical values of  $R$  (0.125 inch), the surface strain would be less than 1 percent. Therefore, the force necessary to propagate a tear will determine the effect of substrate deflection on service life of sealants in a fillet joint.

\*Boeing's deflection simulator.

In addition to dependence on the magnitude of the sealant deformation and the joint configuration, the stress resulting from changes in relative position of the substrate depends on the rate of the change. Since stress relaxation reduces stresses in the material, the larger the rate of stress relaxation, the lower are the stresses imposed on the adhesive joints from joint deflection. However, the more rapid the joint deflection, the greater will be the stresses imposed on the sealant. The converse will be true for the ultimate elongation.

The ultimate elongation will decrease at lower deformation rates and longer times. Thus cohesive rupture will occur at low deformation rates or low strains over a long period of time, while adhesive ruptures will occur at high deformation rates.

#### Temperature Induced Strains for Both Joint Configurations

Temperature is an important parameter in predicting the service life of sealants. The rheological properties of polymers change exponentially with temperature. Properties such as strength and ultimate elongation, however, go through maxima as temperature is varied. One possible source of failure is the difference between the thermal-expansion coefficient of the sealant and that of the substrate.

The thermal-expansion coefficient of the Ti-6Al-4V alloy is about  $9 \times 10^{-6}/C$ , for some silicone elastomers and filled rubbers it is  $\sim 2 \times 10^{-4}/C$ , while that for high-modulus materials is  $\sim 7 \times 10^{-4}/C$ . The strain produced on a polymer in this situation can be estimated readily. Assume that a polymer is applied over a substrate of length  $L_0$ . The strain produced by the temperature change  $\Delta T$  will be the difference between the length that the sample would attain if heated and the length to which it is constrained by the adhesive bond, i. e.,

$$\epsilon = \left| k_M \Delta T \cdot L_0 - k_P \cdot \Delta T \cdot L_0 \right| / L_0 (1 + k_P \Delta T), \quad (20)$$

where  $k_M$  and  $k_P$  are the linear expansion coefficients of the metal and polymer respectively. This simplifies to

$$\epsilon = \Delta T \left| k_M - k_P \right| \sim \Delta T \cdot k_P, \quad (21)$$

since  $k_P \gg k_M$  and  $1 \gg k_P \Delta T$ . Thus, the strain is directly proportional to the linear expansion coefficient of the polymer. For medium- to low-modulus materials stress relaxation along with a reduction in the modulus due to temperature will reduce the stress produced by raising the temperature. A decrease from 25 C to -50 C, the predicted lower service temperature, will produce a strain

$$\epsilon = 75 \times 2 \times 10^{-4} = 1.5 \text{ percent},$$

which is not expected to cause cohesive failure. However, since the modulus increases as the temperature decreases, the shear stress due to this elongation can be as large as 1000 psi. The stress magnitude will depend on the stress relaxation coupled with the

rate of cooling. For high-modulus materials, stress relaxation is small except at high temperatures (where degradation occurs) and significant stresses will be caused by temperature changes independent of time. For example, assume a cure of the high-modulus material at 150 C. Cooling to -50 C will produce a  $\Delta T$  of 200; for a modulus of  $10^5$  psi, e.g., an epoxy resin, the shear stress on the surface will be

$$\sigma = \Delta T \cdot \left| k_P - k_M \right| \cdot G = 200 (7 \cdot 10^{-5} - 9 \cdot 10^{-6}) \cdot 10^5 = 1220 \text{ psi} ,$$

which is appreciably larger than the 500 psi lap shear strength suggested in the RFQ. Therefore, since temperature cycling is effected in service, properties of the sealant must be appreciably different than those assumed, i.e., lap shear  $> 500$  psi,  $G > 10^5$ , or  $k_P \sim k_M$ .

The temperature at which the sealant is cured, especially for sealants with a low relaxation, becomes an important factor in the possible adhesive failure of a sealant. When the mechanical strains from motion of the fuel tank are imposed on these strains, then the stress levels become even larger.

If one portion of the fuel tank is cooler than another, such as the part under liquid fuel in a partially filled tank, then expansion of metal parts can cause a significant shear strain. For example, assume that the top of the tank, because of air friction, is at 225 C and the bottom in contact with the fuel is at 150 C. The difference in expansion will cause a compressive load on the top structure and tensile load on the bottom. If the length of the tank structure is  $L$  and contains  $N$  seams, then the observed strain per joint will be

$$\epsilon = k_M \Delta T L / (2NH) ,$$

where  $H$  is the substrate separation shown in Figure 22. The 2 in the denominator arises from the length being divided between the top and bottom with both having the same number of seams. For a joint every 50 inches and an  $H$  of  $10^{-2}$  inch,  $\epsilon = 1.7$  or 170 percent. Couple this with a 50 percent strain due to motion of the wing structure and the resulting total strain is great enough to cause cohesive failure for all three sealants in a faying sealant and start a crack in the fillet sealant after 40 hours.

### CONCLUSIONS AND RECOMMENDATIONS

The primary objective, the development of a short-term test method to predict the service life of sealants for fuel tanks for advanced aerospace vehicles, has not been achieved in the current program. However, much has been learned regarding typical commercially available sealants with respect to their performance under specified environmental conditions. The following results were obtained during the course of this program:

- (1) Analysis of the effects of joint and sealant configuration, fuel, and temperature on sealant performance has provided criteria that are expected to be useful as a basis for predicting service life of sealants.



- (2) This analysis has shown that the problem is more complex than anticipated, and will require the acquisition of considerably more data before reliable service-life predictions can be made.
- (3) The rheological characteristics of the three sealants studied in this program varied widely and showed that the mechanisms responsible for the changes in these characteristics are different for each one.
- (4) None of the commercially available sealants can be expected to have more than a few hours useful service life in anticipated actual SST flight conditions.

The analysis of the joint configurations with respect to the physical and rheological properties of available sealants has shown that the effects of volume and temperature changes along with the mechanical deformations of the fuel-tank substrate can result in adhesive or cohesive cracks in these sealants. Such cracks may or may not be large enough to cause a fuel leak. Because such cracks may propagate at some lower load, this becomes the predominant mode of failure. Therefore, measurement of aging and

temperature effects on the crack propagation should be considered for use in service-life predictions. This adds to the complexities that have already been recognized in characterizing the behavior of sealants. Whether or not rheological properties alone can be used to predict the service life of sealants for advanced aerospace vehicles becomes questionable. Therefore, it is Battelle's recommendation that continued research in this area involve:

- (1) Continuation of the study of the rheological characteristics of sealants as affected by environment (both fuel and temperature) type of stress or strain and time
- (2) Investigation of simulated service tests that will include the known service requirements of temperature, time, environment, and loading:
  - (a) The Boeing Deflection Simulation Test is expected to be useful to define actual performance
  - (b) The cyclic pressure cell-type simulation suggested by Battelle employs a lap joint in a titanium tubing specimen. This specimen has the advantage that many conditions can be studied including the conditions of fuel and fuel vapor under pressure.

It is suggested that this program be renewed at a rate of effort that will allow both areas of investigation to be conducted simultaneously. It is estimated that considerable progress can be made to achieve the intended goal if the renewal can be funded to include 15 to 18 man-months of research engineer and/or scientist level of effort, with the equivalent support effort employed in the current program.

APPENDIX A

A-1

TABLE A-1.

CERTIFICATE OF ANALYSIS

July 26, 1968

I, Arnold M. Leas, certify that I am employed by Ashland Oil and Refining Company as Director of Research and Development and did observe the following test data on Mil-J-5161F Referee Jet Fuel, Grade II. This certified analysis is applicable to all deliveries from Batch 1 at Covington, Kentucky.

COVINGTON 309 TANK - REFEREE GRADE II MIL-J-5161F

	<u>Specification</u>	<u>Batch 1 309 Tank Covington, Ky. (7-26-68)</u>
Distillation:		
IPB, °F	Report	346
10% Evaporated, °F	400 max	375
20% Evaporated, °F	385-415	389
50% Evaporated, °F	410-440	419
90% Evaporated, °F	460-500	482
EP, °F	550 max	550
Residue, volume %	1.5 max	1
Loss, volume %	1.5 max	0
Gravity, °API	36-43	40.6
Existent Gum, mg./100 ml	7 max	0.8
Potential Gum, mg./100 ml	14 max	4.2
Sulfur, total, weight %	0.30-0.40	0.32
Mercaptan Sulfur, weight %	0.005 max	0.0006
Freezing Point, °F	-40 max	-54
Net Heat of Combustion		
Btu/lb. or	18,300-18,600	18,491
Aniline-Gravity Product	4,500-6,000	5,887
Aromatics, volume %	10-25	17.6
Olefins, volume %	5 max	2.5
Smoke Point, mm	17-21	19
Copper Strip Corrosion	1 max	1(a)
Water Reaction	1(b) max	1
Viscosity, cs at -30°F	10-16.5	10.09
Flash Point, °F	120 min	130
Water Separometer Index Modified	Report	98
Thermal Stability, 300/400/6		
ΔP Inches Hg in 5 Hours	15 max	2.4
Preheater Deposit	3 max	1

ASHLAND OIL &amp; REFINING COMPANY

*Arnold M. Leas*  
 \_\_\_\_\_  
 Arnold M. Leas, Director  
 Research and Development Department

TABLE A-2. EFFECT OF AGING ON TENSILE PROPERTIES OF VITON SEALANT  
Aged at Elevated Temperatures in Various Environments

Temperature, C	Hours Aged	Slope		Stress at Indicated Elongation, psi		Ultimate	
		Initial	Final	50%	100%	Stress, psi	Elongation, %
<u>Air Aging</u>							
Initial	0	1194	117	157	190	252	1.63
		1042	117	148	226	406	2.80
		1061	187	186	234	507	2.50
150	4	1095	158	150	192	402	2.33
		971	78	142	175	184	1.12
		1034	173	161	204	477	2.65
	40	855	154	146	189	405	2.52
		885	137	140	179	383	2.50
		1024	180	129	173	397	2.30
	400	1107	144	160	207	367	2.18
		1038	141	155	204	355	2.11
		1282	140	140	183	357	2.20
200	4	--	--	--	--	--	--
		1013	146	146	186	372	2.37
		880	180	165	211	469	2.45
	40	848	153	151	196	371	2.20
		848	140	144	189	373	2.38
		757	274	148	223	474	1.95
	400	757	158	115	169	255	1.63
		711	153	121	192	202	1.06
		974	189	132	187	343	1.91
250	4	969	140	152	194	290	1.73
		953	149	143	184	388	2.15
		1070	189	165	217	444	2.25
	40	1061	212	155	233	401	1.88
		1036	183	160	232	353	1.73
		930	259	163	246	427	1.75
	400	1347	472	237	459	687	1.54
		1468	367	265	455	534	1.31
		1471	441	252	496	579	1.32
<u>Fuel Aging</u>							
150	4	855	117	115	149	381	2.99
		864	104	107	138	368	3.14
		790	165	134	176	463	2.65
	40	676	114	108	142	338	2.55
		672	113	102	136	345	2.85
		450	143	108	149	398	2.80
	400	731	126	108	147	351	2.71
		800	121	117	150	368	2.84
		1008	129	103	134	324	2.60

TABLE A-2. (Continued)

Temperature, C	Hours Aged	Slope		Stress at Indicated Elongation, psi		Ultimate			
		Initial	Final	50%	100%	Stress, psi	Elongation, %		
200	4	777	111	103	131	341	2.79		
		717	115	102	133	245	1.90		
		689	149	123	141	400	2.80		
	40	620	105	95	129	257	2.30		
		463	102	90	125	301	2.68		
		498	137	100	141	309	2.20		
	400	558	178	98	159	224	1.39		
		728	182	115	182	246	1.37		
		604	188	101	169	217	1.26		
250	4	742	98	113	134	295	2.78		
		584	103	105	128	292	2.73		
		547	129	112	138	314	2.50		
	40	726	136	114	165	267	1.80		
		611	135	108	155	234	1.61		
		346	181	103	165	258	1.60		
	400	1522	350	--	--	226	0.37		
		Cracked	--	--	--	--	--		
		1415	234	--	--	196	0.28		
150	4	<u>Vapor Aging</u>		1076	121	128	158	375	2.79
		668	132	132	168	407	2.84		
		778	165	152	198	396	2.25		
	40	585	131	116	155	329	2.38		
		681	123	111	148	308	2.38		
		418	165	117	163	402	2.55		
	400	634	102	97	124	316	2.98		
		607	98	101	128	315	2.96		
		828	136	94	122	309	2.73		
200	4	--	--	111	131	317	2.90		
		729	96	114	136	329	3.08		
		971	101	114	130	346	3.35		
	40	588	107	101	130	271	2.36		
		584	98	102	133	225	2.03		
		509	114	96	127	321	2.90		
	400	731	168	107	160	308	1.86		
		754	166	114	169	330	1.96		
		744	164	95	142	314	2.12		
250	4	--	--	--	--	303	2.74		
		688	108	108	130	291	2.52		
		661	125	112	136	327	2.70		
	40	799	186	140	207	315	1.52		
		690	191	130	196	295	1.55		
		771	346	171	281	347	1.50		
	400	1243	162	--	--	369	0.24		
		Cracked	--	--	--	--	--		
		Damaged	--	--	--	--	--		

TABLE A-3. EFFECT OF AGING ON STRESS RELAXATION OF VITON SEALANT  
Aged at Elevated Temperatures in Various Environments

Temperature, C	Hours Aged	Strain, in./in.	Modulus at 0.05 Min	Slope at 0.05 Min	Modulus at 9 Min	Slope <sup>(a)</sup>	Slope at 9 Min
<u>Air Aging</u>							
Initial	0	0.240	303	8306	202	-0.0859	67.4
		0.236	368	5109	229		145
150	4	0.228	308	3750	208	-0.0905	122
		0.258	342	9155	198		102
	40	0.221	339	7490	217	-0.089	73.0
		0.225	372	10254	231		104
	400	0.212	323	6773	208	-0.083	10.8
		0.212	329	6426	216		14.5
200	4	0.240	330	7079	209	-0.0902	51.5
		0.233	353	9303	218		80.1
	40	0.277	272	5347	163	-0.0972	33.6
		0.277	263	5085	160		37.4
	400	0.172	242	7933	135	-0.119	13.0
		0.176	261	8242	136		13.2
250	4	0.219	316	13400	193	-0.0898	92.7
		0.214	335	8880	215		167
	40	0.165	338	10471	187	-0.110	63.1
		0.165	306	9154	176		48.1
	400	0.133	428	17150	181	-0.166	27.7
		0.133	423	16070	177		19.3
<u>Fuel Aging</u>							
150	4	0.252	257	5364	164	-0.092	27.6
		0.258	275	5478	166		43.0
	40	0.265	194	3780	116	-0.0952	30.1
		0.269	216	3694	134		33.4
	400	0.245	218	5902	138	-0.0898	9.2
		0.246	262	5631	163		9.9
200	4	0.241	261	5606	152	-0.108	29.2
		0.241	254	7011	142		17.2
	40	0.201	188	5394	112	-0.0996	78.7
		0.205	193	4713	115		28.2
	400	0.131	235	6970	135	-0.106	12.1
		0.127	267	7828	154		12.6
250	4	0.242	233	6733	123	-0.121	39.2
		0.240	192	5668	103		49.1
	40	0.147	226	5973	121	-0.123	60.4
		0.148	229	6263	119		70.3
	400	0.057	650	21795	263	-0.192	47.4
		0.059	667	25641	223		48.7

TABLE A-3. (Continued)

Temperature, C	Hours Aged	Strain, in./in.	Modulus at 0.05 Min	Slope at 0.05 Min	Modulus at 9 Min	Slope <sup>(a)</sup>	Slope at 9 Min	
<u>Vapor Aging</u>								
150	4	0.211	276	5301	177	-0.089	42.1	
		0.213	303	6635	188		42.3	
	40	0.238	259	4672	158	-0.0927	36.3	
		0.237	225	4343	141		36.1	
	400	0.261	201	5882	120	-0.1011	9.9	
		0.261	212	5692	124		9.2	
200	4	0.314	224	5650	117	-0.125	28.0	
		0.318	222	9877	116		24.7	
	40	0.274	193	4930	101	-0.124	35.1	
		0.274	189	5045	99		1.9	
	400	0.226	225	7273	130	-0.107	10.2	
		0.194	242	5833	138		10.0	
250	4	0.248	240	7173	127	-0.121	39.5	
		0.260	223	5486	119		39.2	
	40	0.131	300	8429	163	-0.118	48.1	
		0.133	311	8045	167		70.6	
	400	Tore						

(a) Slope of the Log Modulus - Log Time Plot.

TABLE A-4. EFFECT OF AGING ON TENSILE PROPERTIES OF DOW CORNING SEALANT 94-030

Aged at Elevated Temperatures in Various Environments

Temperature, C	Hours Aged	Slope		Stress at Indicated Elongation, psi		Ultimate	
		Initial	Final	50%	100%	Stress, psi	Elongation, %
<u>Air Aging</u>							
Initial	0	524	236	112	196	554	2.70
		449	213	113	203	599	2.88
150	4	445	213	107	194	379	1.96
		336	221	115	209	614	2.90
		423	212	113	205	636	3.02
	40	453	226	118	212	671	3.08
		520	201	112	195	343	1.76
		537	245	131	230	654	2.82
200	4	431	207	119	207	520	2.61
		507	221	121	217	676	3.17
		436	203	112	201	442	2.22
	40	484	230	125	226	641	2.88
		460	246	125	230	623	2.67
		452	238	130	247	358	1.50
250	4	426	213	121	216	591	2.78
		422	213	117	209	410	1.97
		533	221	124	217	599	2.76
	40	455	227	121	220	515	2.33
		525	206	123	216	446	2.12
		446	240	129	246	466	1.92
<u>Fuel Aging</u>							
150	4	321	198	98	180	523	2.75
		389	220	106	196	498	2.39
		406	194	104	190	531	2.80
	40	151	123	66	124	273	2.23
		246	123	68	126	315	2.48
		316	123	64	124	260	2.01
200	4	311	187	92	171	339	1.88
		311	185	88	169	369	2.05
		277	190	88	167	404	2.27
	40	42	80	9.1	22.6	181	3.11
		29	91	15.2	37.8	204	3.40
		Too soft					
250	4	156	115	53	106	209	1.89
		165	142	67	126	321	2.32
		243	130	61	120	234	1.85
	40	Too soft					



TABLE A-4. (Continued)

Temperature, C	Hours Aged	Slope		Stress at Indicated Elongation, psi		Ultimate	
		Initial	Final	50%	100%	Stress, psi	Elongation, %
<u>Vapor Aging</u>							
150	4	451	208	105	188	586	2.97
			209	99	195	669	3.27
		375	177	101	181	316	1.76
	40	399	225	115	207	636	3.03
		401	209	114	204	583	2.86
		400	207	113	202	562	2.81
200	4	285	201	52	87	531	2.90
		388	194	107	188	440	2.31
		448	210	109	192	613	3.23
	40	255	143	78	147	321	2.26
		323	170	99	173	407	2.49
		302	139	82	150	296	2.02
250	4	173	130	69	134	367	2.71
		268	127	68	131	351	2.77
		227	134	75	139	380	2.86
	40	Too soft					

TABLE A-5. EFFECT OF AGING ON STRESS RELAXATION OF DOW CORNING SEALANT 94-030

Aged at Elevated Temperatures in Various Environments

Temperature, C	Hours Aged	Strain, in./in.	Modulus at 0.05 Min	Slope at 0.05 Min	Modulus at 5 Min	Slope(a)	Slope at 5 Min
<u>Air Aging</u>							
Initial	0	0.289	218	801	198	-.0186	7.37
		0.297	211	641	191		8.31
		0.284	199	665	187		6.96
150	4	0.330	191	677	177	-.0167	4.71
		0.328	201	798	186		8.48
	40	0.276	219	768	187	-.0263	11.4
		0.275	216	681	198		8.2
200	4	0.230	223	883	204	-.0133	10.4
		0.230	218	818	201		5.8
	40	0.153	244	767	227	-.0160	10.7
		0.153	248	932	230		7.4
250	4	0.277	209	888	191	-.0181	14.6
		0.277	199	725	184		5.6
	40	0.182	207	638	193	-.0148	4.2
		0.181	219	655	205		2.62
<u>Fuel Aging</u>							
150	4	--					
		--					
	40	0.204	116	628	103	-.0253	5.86
200	4	0.203	104	484	93		2.95
		0.230	164	697	151	-.0190	5.07
	40	0.230	156	634	142		5.25
			Too soft				
250	4	--					
		0.187	89	457	80	-.0233	4.35
	40	0.187	97	489	87		3.91
			Too soft				
<u>Vapor Aging</u>							
150	4	0.178	217	639	202	-.0167	3.95
		0.178	213	694	196		7.79
	40	0.278	198	876	182	-.0176	7.37
		0.283	194	930	179		4.34
200	4	0.311	111	655	100	-.0224	2.70
		0.316	175	708	158		4.66
	40	0.206	127	987	111	-.0238	3.15
		0.205	154	882	141		5.80
250	4	0.285	111	862	98	-.0295	3.78
		0.282	109	855	94		4.79
	40		Too soft				
--							

(a) Slope of the Log Modulus - Log Time Plot.

TABLE A-6. EFFECT OF AGING ON TENSILE PROPERTIES OF DOW CORNING SEALANT 94-516

Aged at Elevated Temperatures in Various Environments

Temperature, C	Hours Aged	Slope		Stress at Indicated Elongation, psi		Ultimate	
		Initial	Final	50%	100%	Stress, psi	Elongation, %
<u>Air Aging</u>							
Initial	0	121	209	65.5	149	421	2.28
		102	212	52.2	135	499	2.70
		179	293	73.2	175	457	2.07
150	4	31	94	16.3	40	348	4.42
		132	207	73.1	156	301	1.69
		113	214	57.0	136	403	2.34
	40	116	235	60.7	138	290	1.72
		108	257	56.0	141	394	2.07
		191	186	61.2	144	155	1.08
200	4	121	241	62.9	149	470	2.39
		121	242	68.8	155	574	2.74
		123	273	62.3	150	511	2.39
	40	144	257	76.1	183	308	1.50
		164	267	86.4	195	382	1.68
		210	326	92.2	220	624	2.18
250	4	112	243	60.4	146	400	2.08
		113	254	64.8	153	414	2.04
		127	292	63.8	157	498	2.30
	40	171	294	58.4	213	376	1.55
		160	303	91.9	212	434	1.84
		225	352	86.8	214	434	1.69
<u>Fuel Aging</u>							
150	4	111	207	58.6	133	391	2.45
		100	219	52.4	123	476	2.65
		105	241	63.0	143	508	2.63
	40	133	184	71.2	154	208	1.32
		114	241	60.9	137	439	2.36
		226	261	68.2	161	414	2.04
200	4	101	208	55.3	123	352	2.09
		106	199	54.5	128	385	2.31
		98	204	54.5	124	358	2.16
	40	114	224	60.1	139	401	2.19
		106	247	56.0	133	478	2.50
		88	180	44.3	109	168	1.33

TABLE A-6. (Continued)

Temperature, C	Hours Aged	Slope		Stress at Indicated Elongation, psi		Ultimate	
		Initial	Final	50%	100%	Stress, psi	Elongation, %
250	4	95	186	50.5	116	307	2.06
		90	206	48.8	112	446	2.84
		16	63	8.35	20.9	192	3.63
	40	--					
		--	18	62	13.6	36.1	78.2
150	4						
		Vapor Aging					
		99	212	51.0	125	404	2.32
	114	225	59.4	142	300	1.72	
	106	236	52.4	125	462	2.59	
	40	110	214	57.9	139	322	1.91
102		216	52.5	128	369	2.14	
140		269	65.6	162	382	1.88	
200	4	111	208	58.7	136	451	2.54
		113	207	58.5	138	426	2.35
		113	243	64.2	148	507	2.68
	40	83	141	42.6	104	122	1.13
		112	244	57.5	131	512	2.73
		167	241	63.6	150	350	1.82
250	4	74	206	39.8	104	487	3.18
		71	209	35.4	84.6	383	2.59
		65	179	36.2	90.2	323	2.38
	40	18	41	9.03	18.5	127	4.06
		20	36	9.94	13.2	134	4.80
		17	23	4.35	10.0	60.8	3.67

TABLE A-7. EFFECT OF AGING ON STRESS RELAXATION OF DOW CORNING SEALANT 94-516

Aged at Elevated Temperatures in Various Environments

Temperature, C	Hours Aged	Strain, in./in.	Modulus at 0.05 Min	Slope at 0.05 Min	Modulus at 5 Min	Slope(a)	Slope at 5 Min
<u>Air Aging</u>							
Initial	0	0.210	108	166	105	-.0073	1.29
		0.204	108	189	104		1.33
150	4	0.234	24.9	231	22.3	-.0053	0.627
		0.233	132	231	129		0.444
	40	0.140	99	180	96	-.00885	0.838
		0.115	122	289	116		2.96
200	4	0.241	111	322	108	-.0066	0.383
		0.243	122	222	118		0.638
	40	0.220	133	250	130	-.00485	0.808
		0.220	140	178	137		0.828
250	4	0.233	116	275	111	-.0093	1.10
		0.234	121	240	116		1.44
	40	0.167	153	362	147	-.0084	0.724
		0.168	134	339	129		1.46
<u>Fuel Aging</u>							
150	4	0.264	107	197	105	-.0053	0.346
		0.252	105	264	102		0.321
	40	0.206	134	151	131	-.0044	0.734
		0.205	119	213	117		0.766
200	4	0.219	103	311	100	-.00615	0.155
		0.225	102	248	99		0.147
	40	0.138	123	248	117	-.0109	0.497
		0.137	120	283	114		0.189
250	4	0.391	88	291	86	-.00795	0.560
		0.392	81	347	77		0.572
	40	0.277	17.0	233	14.2(c)	-.0512(b)	1.24(c)
		0.277	21.0	226	17.3(c)		1.24(c)
<u>Vapor Aging</u>							
150	4	0.261	97	94	95	-.0064	1.63
		0.256	112	303	108		0.840
	40	0.188	105	220	101	-.0084	0.617
		0.190	110	205	106		1.02
200	4	0.271	94	108	92	-.0066	0.836
		0.271	102	324	98		0.957
	40	0.182	91	258	87	-.00975	1.36
		0.184	110	321	105		1.90
250	4	0.246	76	273	73	-.00885	0.988
		0.235	73	251	70		0.635
	40	0.375	10.3	217	7.4	-.00866	0.338
		0.365	6.7	170	4.0		0.194

(a) Slope of the Log Modulus - Log Time Plot.

(b) At .05 - 2 min.

(c) At 2 min (these 2 samples only).

APPENDIX E

TORSIONAL DAMPING EQUATIONS

B-1

APPENDIX B

TORSIONAL DAMPING EQUATIONS

The torsional damping equations for amplitudes within the linear range are the same as have been derived from the well-known ones for damped simple harmonic motion. In the model illustrated in Figure B-1,  $k$  is the spring constant,  $\eta$  the viscosity

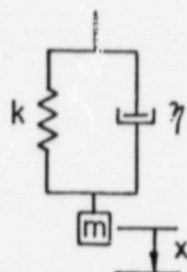


FIGURE B-1. MODEL FOR DAMPED HARMONIC MOTION

(or damping) constant, and  $m$  the mass. When the mass is given displacement  $x$  and released, the system will oscillate with a constant frequency decreasing in amplitude, as shown in Figure 8. The differential equation for this motion is given by

$$F_m = F_s + F_\eta \quad ; \quad m \frac{d^2x}{dt^2} = \eta \frac{dx}{dt} - kx \quad (B-1)$$

where  $F_m$  is the force exerted on the mass,  $F_s$  is the force exerted by the spring, and  $F_\eta$  is the force exerted by the dashpot.

There are three possible solutions to this equation. The first is the critical damping case, which applies when

$$\eta = 2 \sqrt{km} \quad . \quad (B-2)$$

The second is that for overdamping. This, like the first case, prevents free oscillation from occurring, and applies when

$$\eta > 2 \sqrt{km} \quad . \quad (B-3)$$

The third case is the one we are interested in, and is applicable when

$$\eta < 2 \sqrt{km} \quad . \quad (B-4)$$

For torsional damping,  $I$ , the moment of inertia is substituted for  $m$ . Condition 3 can always be fulfilled by either increasing  $I$  or  $k$ . With the Rheogoniometer, both  $I$  and  $k$  can be varied.  $k$  is the spring constant of the torsion bar,  $I$  is varied by moving weights along the inertia arm. Therefore, we are assured of fulfilling Condition 3.

B-2

The solution of this equation given by Ferry\* is

$$G' = (2\pi f)^2 (I/b) (1 + \delta^2/4\pi^2) \quad (B-5)$$

$$G'' = (2\pi f)^2 (I/b) (\delta/\pi) \quad (B-6)$$

where  $G'$  is the elastic modulus,  $G''$  is the viscous modulus, and  $b$  is the geometric factor, which for a right cylinder of diameter  $D$  and height  $h$  is

$$b = \pi D^4/32h \quad (B-7)$$

The inertia can be determined from the natural frequency of the torsion system without a sample, and is given by

$$I = k_s/4\pi^2 f_s^2 \quad (B-8)$$

Making the appropriate substitutions we obtain

$$G' = (1.018 \cdot 10^6 k_s \cdot h/D^4) \cdot (f/f_s)^2 \cdot (1 + \delta^2/4\pi^2) \quad (B-9)$$

$$G'' = (1.018 \cdot 10^6 k_s \cdot h/D^4) \cdot (f/f_s)^2 \cdot (\delta/\pi) \quad (B-10)$$

These elastic and viscous moduli include the elastic and viscous moduli of the spring as well as the sample. In order to obtain that of the sample, assume a model such as that shown in Figure B-2, so that

$$G''_T = G'' + G''_s \quad ; \quad G'_T = G' + G'_s \quad (B-11)$$

where subscript T refers to the total modulus and S refers to the modulus due to the spring.

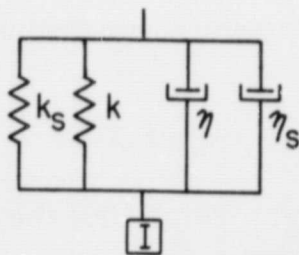


FIGURE B-2. MODEL FOR TORSIONAL DAMPING

\*Ferry, J. D., Viscoelastic Properties of Polymers, Wiley, New York (1961), p. 118.



B-3 and B-4

Using the relations given by Equation (B-11), we obtain

$$G' = (1.018 \cdot 10^6 k_s h/D^4) \cdot [(f/f_s)^2 \cdot (1 + \delta^2/4\pi^2) - (1 + \delta_s^2/4\pi^2)] \quad (B-12)$$

$$G'' = (1.018 \cdot 10^6 k_s h/D^4) \cdot [(f/f_s)^2 \cdot (\delta/\pi) - (\delta_s/\pi)] \quad (B-13)$$

where the subscript s refers to the frequency or decrement of the torsion bar itself.

These equations have been used in a program prepared for the General Electric time-sharing computer service. The output obtained is shown in Table B-1. The Range column indicates the range position on the electronics of the Rheogoniometer, the larger numbers referring to the larger amplitude of oscillation. The number given is the micrometer deflection observed 10 centimeters from the radius of the torsion system; therefore, 2,000 would refer to approximately  $2 \times 10^{-3}$  radians. The decrement, frequency, and time constant have been defined previously. The viscous modulus in the next column is  $G''$  of Equation (B-13), and the elastic modulus is  $G'$  of Equation (B-12). The loss tangent is the ratio of the viscous modulus of the elastic modulus, and is an indication of the ratio of loss to recoverable energy.